Machine Learning the Microscopic Form of Nematic Order in twisted double-bilayer graphene

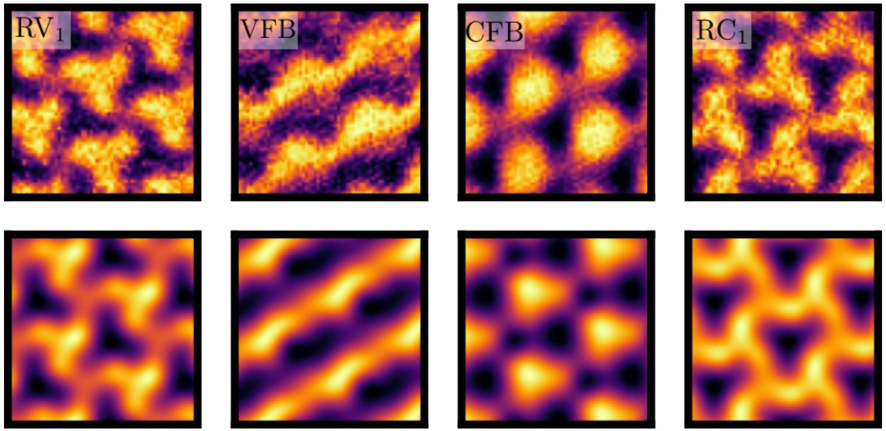

João Augusto Sobral (University of Innsbruck -> University of Stuttgart)

Journal Club for Quantum Physics and Machine Learning (27/06/2023), ultracold.org

arXiv:2302.12274

Acknowledgments

Simon Eli Turkel
Columbia University

Abhay Pasupathy
Columbia University

Stefan Obernauer
University of Innsbruck

Mathias S. Scheurer,
University of Innsbruck →
University of Stuttgart

- Funding by the European Union (ERC-2021-STG, Project 101040651---SuperCorr).
- Discussions with Sayan Banerjee (UIBK), J. P. Valeriano (ICTP-SAIFR/Brazil), Igor Reis (USP/Brazil), Pedro H. P. Cintra (Unicamp/Brazil).

- More information about the slides: joaosds.github.io

Funded by the European Union

Nematicity

TBG: Y. Cao, D. Rodan-Legrain, J. M. Park, N. F. Q. Yuan, K. Watanabe, T. Taniguchi, R. M. Fernandes, L. Fu, and P. Jarillo-Herrero. Science 372, 264 (2021)

$CaFe_2As_2$

Iron-based superconductor

3

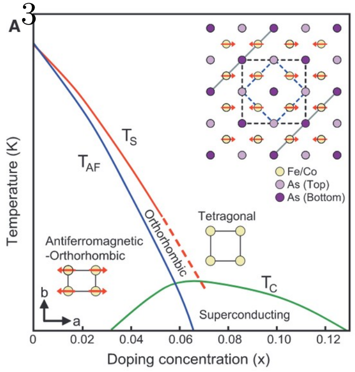

$Bi_2Sr_2CaCu_2O_{8+\delta}$

Copper-oxide superconductors

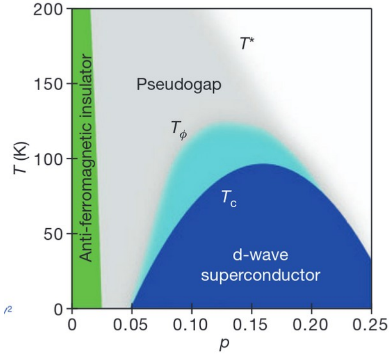

Lawler, M.J. et al, 2010. Nature, 466(7304) | Chuang, T.M, et al , 2010. Science, 327(5962), pp.181-184. | Fernandes, R.M., Chubukov, A.V. and Schmalian, J., 2014. Nature physics, 10(2), pp.97-104.

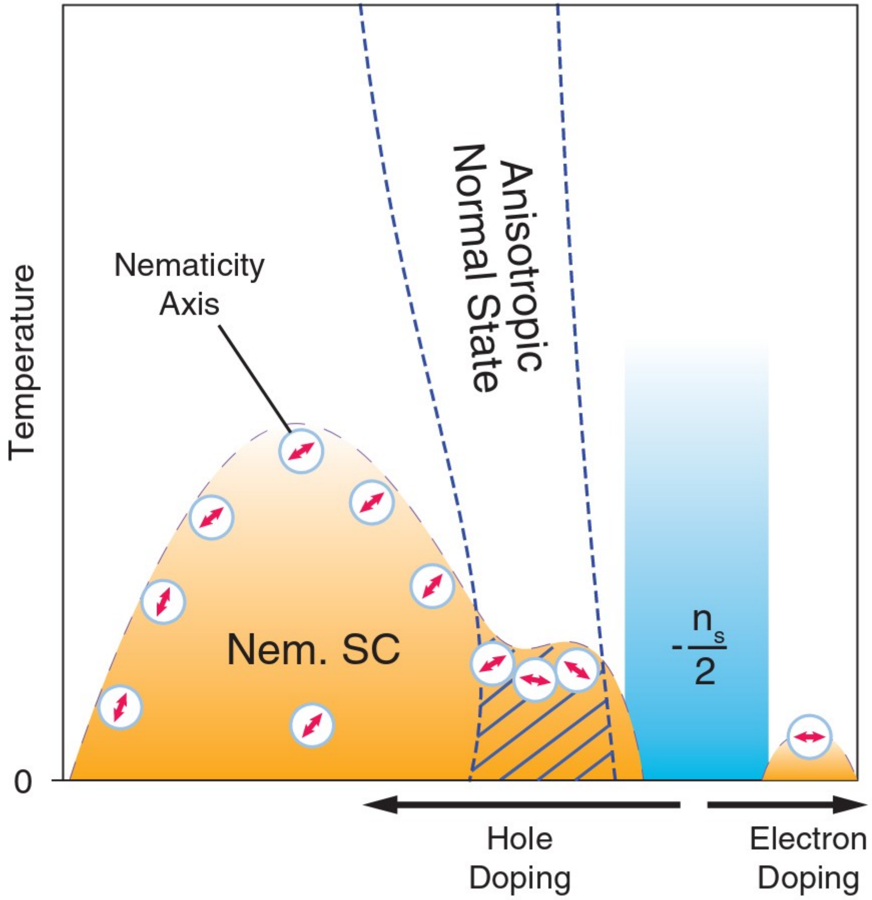

STM

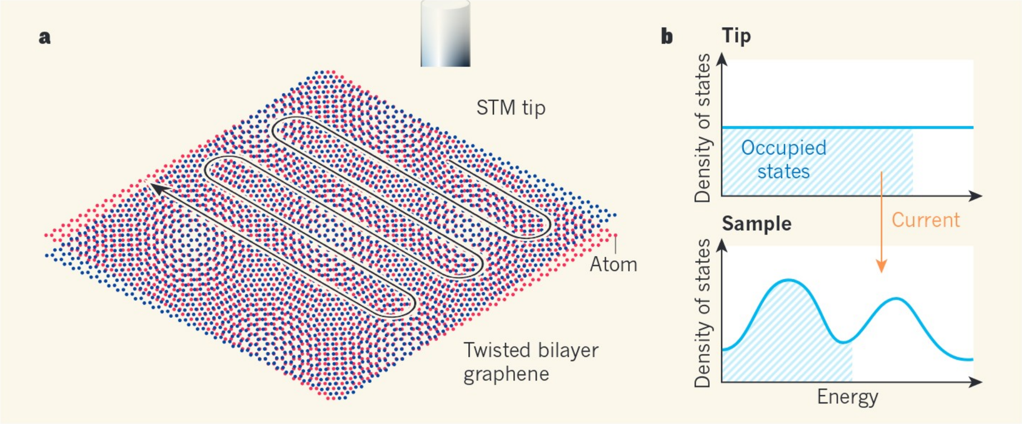

Scheurer, M.S., 2019. Spectroscopy of graphene with a magic twist. Nature, 572(7767), pp.40-41.

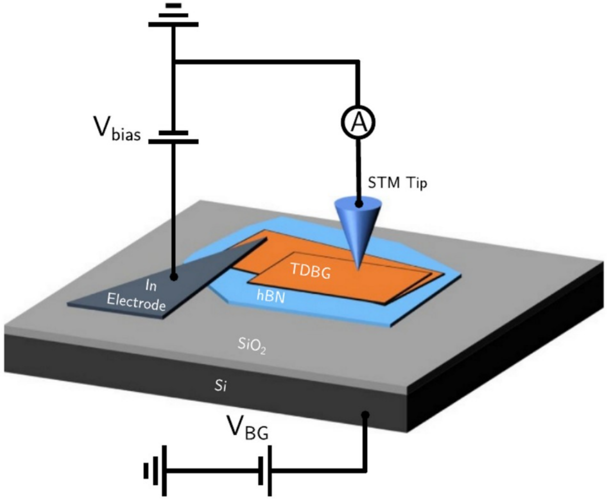

R. Samajdar, M. S. Scheurer, S. Turkel, et al. 2D Materials 8, 034005 (2021).

$$dI/dV \propto \mathcal{D}(\boldsymbol{r}, E)$$

$Bi_2Sr_2CaCu_2O_{8+\delta}$

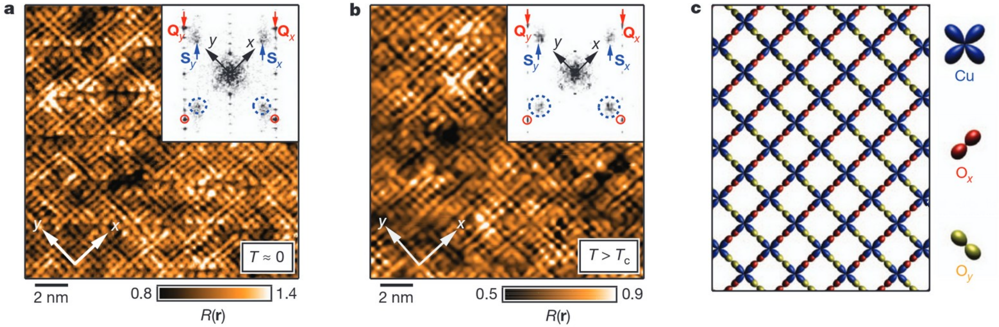

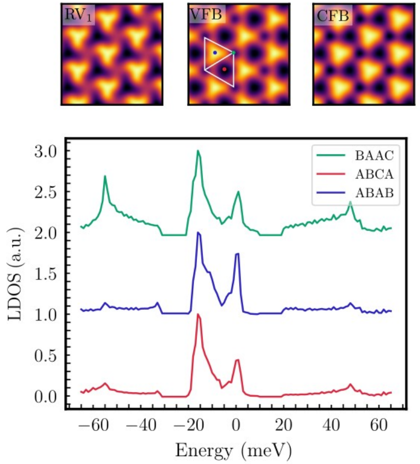

Using AI to detect nematicity

$$
\begin{aligned}
H &= H_0 + H_{imp} \\
H_0 &= -\sum_{\mathbf{r}} t_x c^\dagger_{\mathbf{r}+\hat{x}} c_{\mathbf{r}} + t_y c^\dagger_{\mathbf{r}+\hat{y}} c_{\mathbf{r}} + \text{h.c.} \\
H_{imp} &= \sum_{\mathbf{r}\in R_w} w_{\mathbf{r}} c^\dagger_{\mathbf{r}} c_{\mathbf{r}},
\end{aligned}
$$

$$
O_N = \sum_{\mathbf{r}} N_{\mathbf{r}} \left[\cos(\mathbf{Q}_x \cdot \mathbf{r}) - \cos(\mathbf{Q}_y \cdot \mathbf{r})\right]
$$

DOS ($N_{\mathbf{r}}$)

$$
\mathrm{Q}_x = \left(\tfrac{2\pi}{a}, 0\right) \text{ and } \mathrm{Q}_y = \left(0, \tfrac{2\pi}{a}\right)
$$

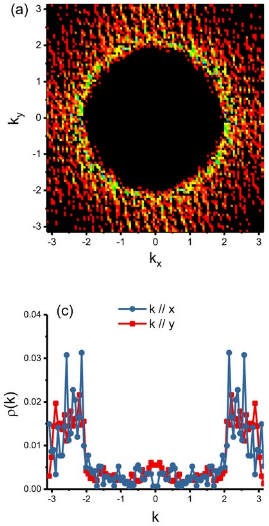

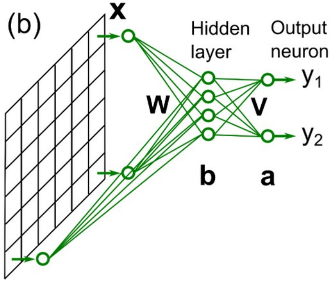

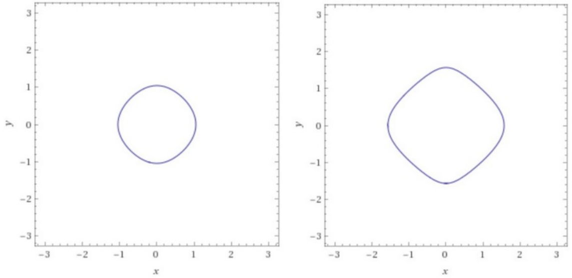

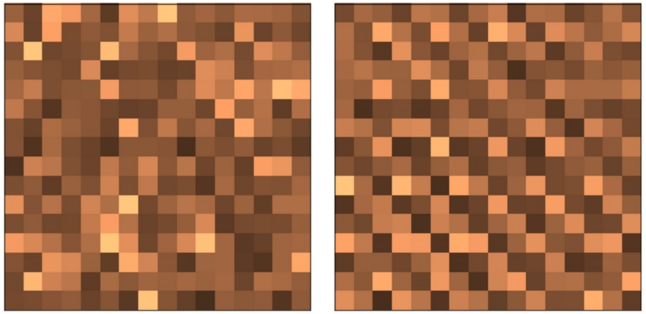

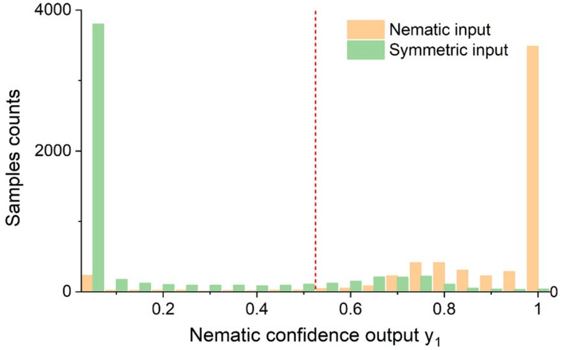

Goetz, J.B., et al **2020**. SciPost Physics, 8(6), p.087.

Using AI to detect nematicity

$CaFe_2As_2$

Goetz, J.B., et al 2020. SciPost Physics, 8(6), p.087.

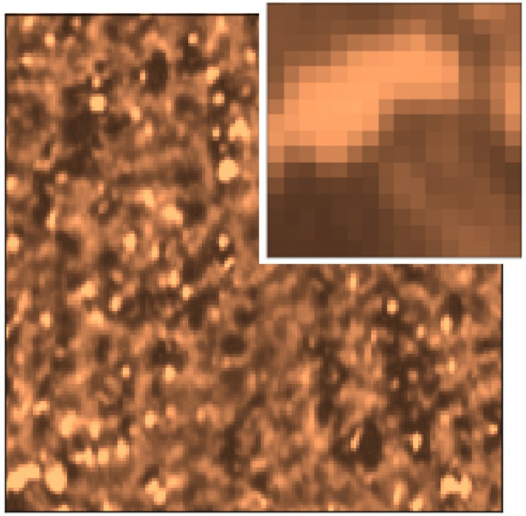

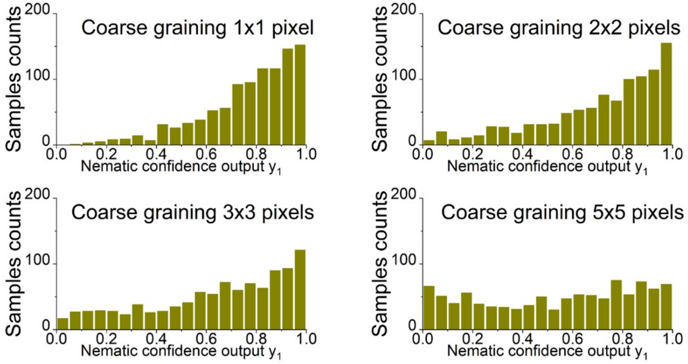

- ~90% exp dataset nematic;
- Need at least one hidden layer - > Non linearity...;
- Disorder in TB model is needed;
- No microscopic form;

Nematicity in TBG

Taranto, W., et al 2022. arXiv preprint arXiv:2203.04449.

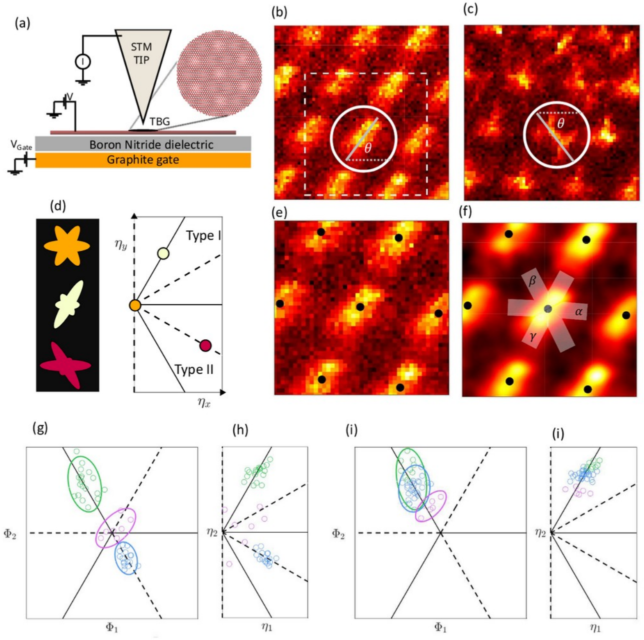

Twisted double-bilayer graphene (TDBG)

$\theta = 1.05°$

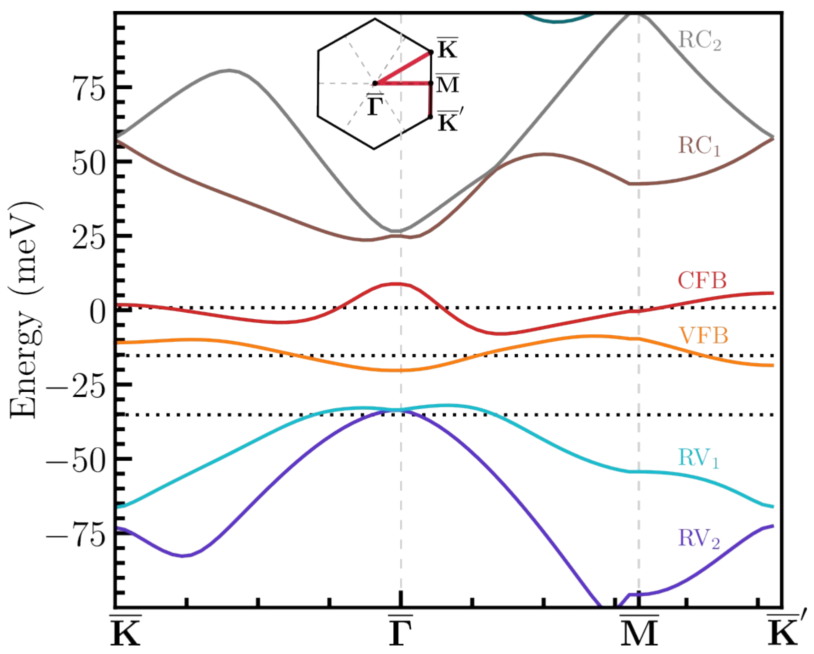

filling fraction of the CFB of $\nu = 0.475$

- Stiffness of bilayer graphene → uniform samples, low strain.

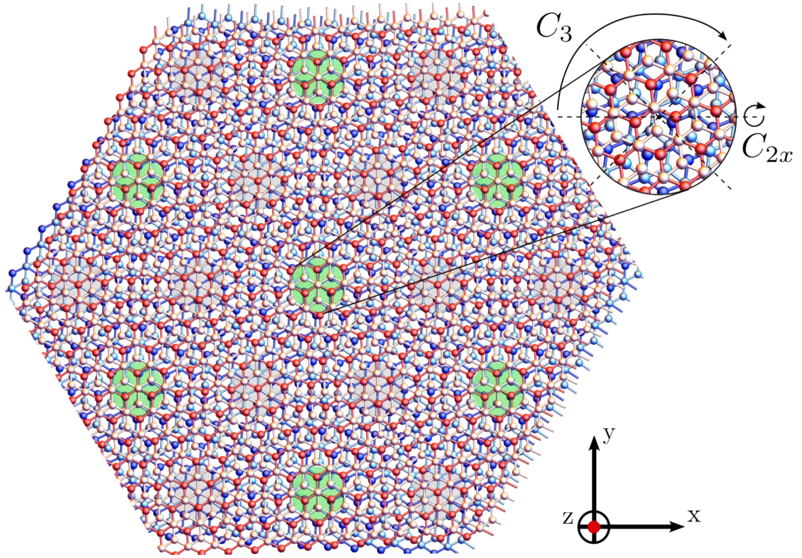

interactions within graphene monolayers

$$H_{AB-AB} = \begin{pmatrix} H_0(\boldsymbol{k}_1) & S^\dagger(\boldsymbol{k}_1) & & \\ S(\boldsymbol{k}_1) & H_0'(\boldsymbol{k}_1) & U^\dagger & \\ & U & H_0(\boldsymbol{k}_2) & S^\dagger(\boldsymbol{k}_2) \\ & & S(\boldsymbol{k}_2) & H_0(\boldsymbol{k}_2') \end{pmatrix} + V$$

interlayer asymetric potential

Moiré interlayer coupling between twisted layers

interlayer coupling of AB stacked BG

Local Density of States (LDOS)

$$\mathcal{D}\left(\boldsymbol{r}, E\right) =$$

$$= \sum_{n,\boldsymbol{k}} \sum_{\boldsymbol{G},\boldsymbol{G}'} e^{-i\left(\boldsymbol{G}-\boldsymbol{G}'\right)} \delta\left(E - E_{n,\boldsymbol{k}}\right)$$

band index

$$\times \left(\left[U^{A_4}_{n,\boldsymbol{k}}\left(\boldsymbol{G}'\right)\right]^* U^{A_4}_{n,\boldsymbol{k}}\left(\boldsymbol{G}\right) + \left[U^{B_4}_{n,\boldsymbol{k}}\left(\boldsymbol{G}'\right)\right]^* U^{B_4}_{n,\boldsymbol{k}}\left(\boldsymbol{G}\right) \right)$$

(LDOS) projected onto 4th graphene layer

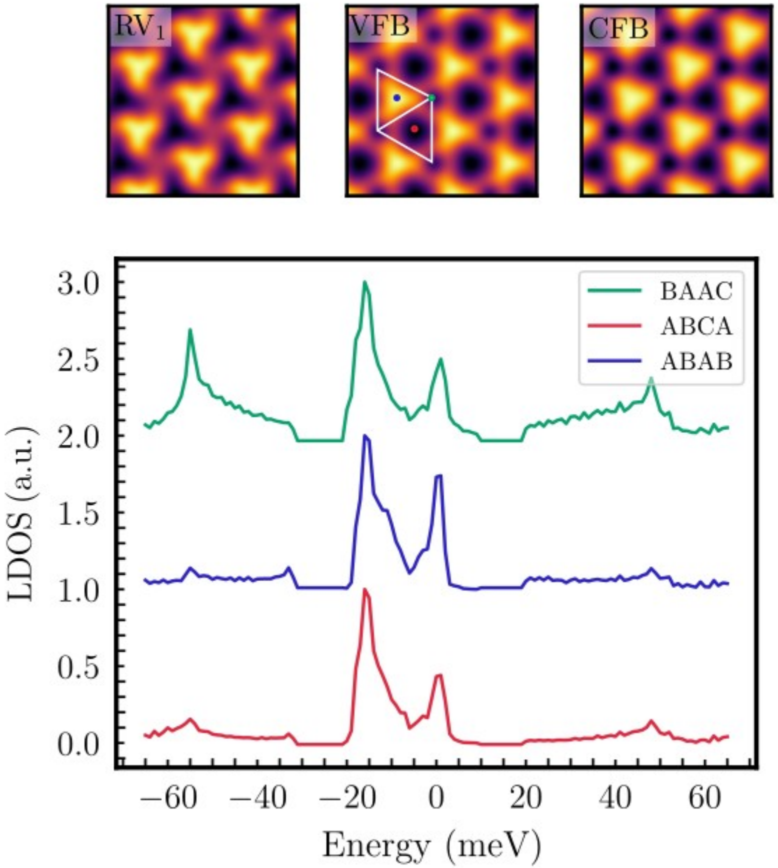

Nematicity in TDBG

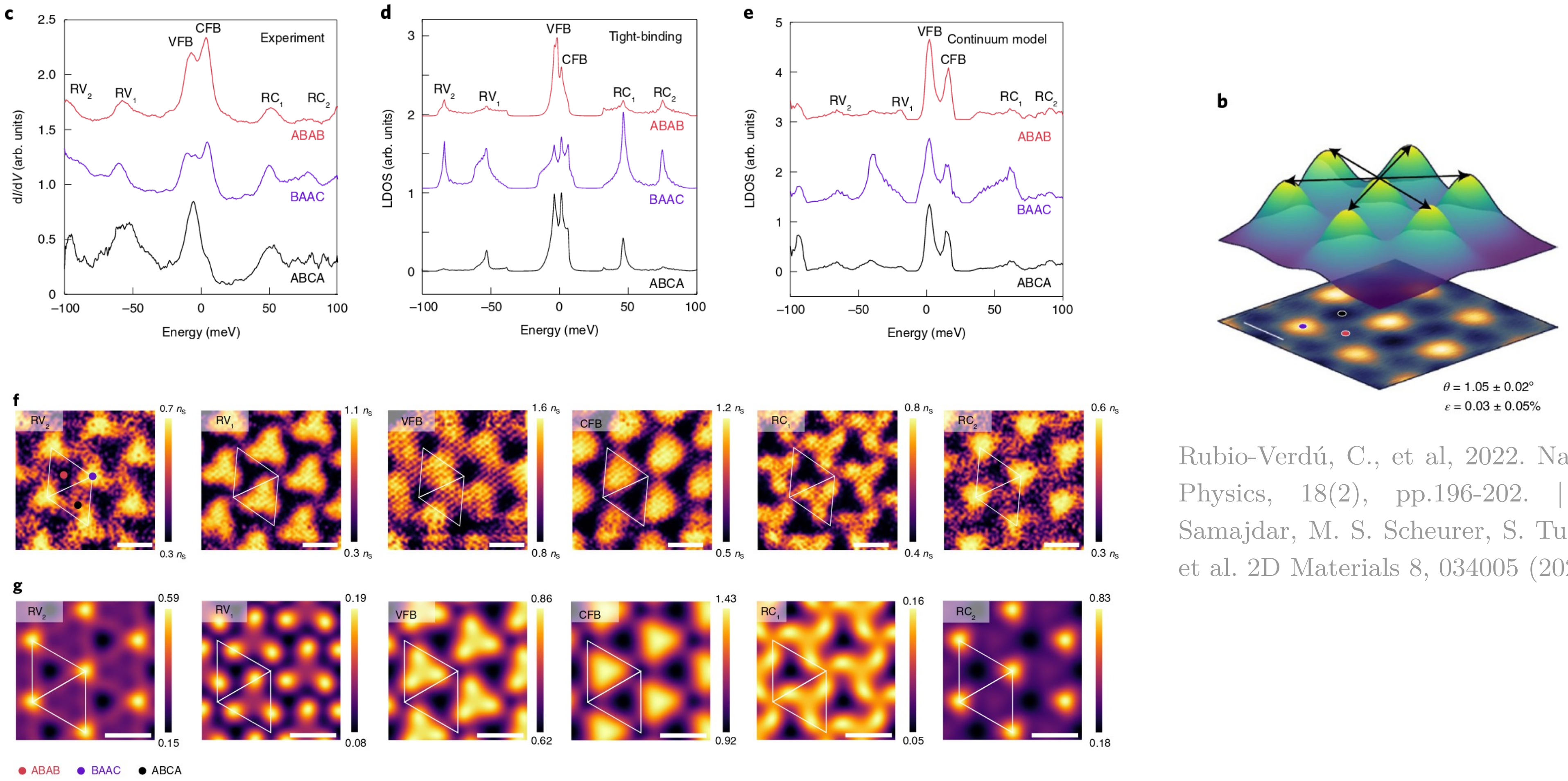

Rubio-Verdú, C., et al, 2022. Nature Physics, 18(2), pp.196-202. | R. Samajdar, M. S. Scheurer, S. Turkel, et al. 2D Materials 8, 034005 (2021).

Nematicity in TDBG

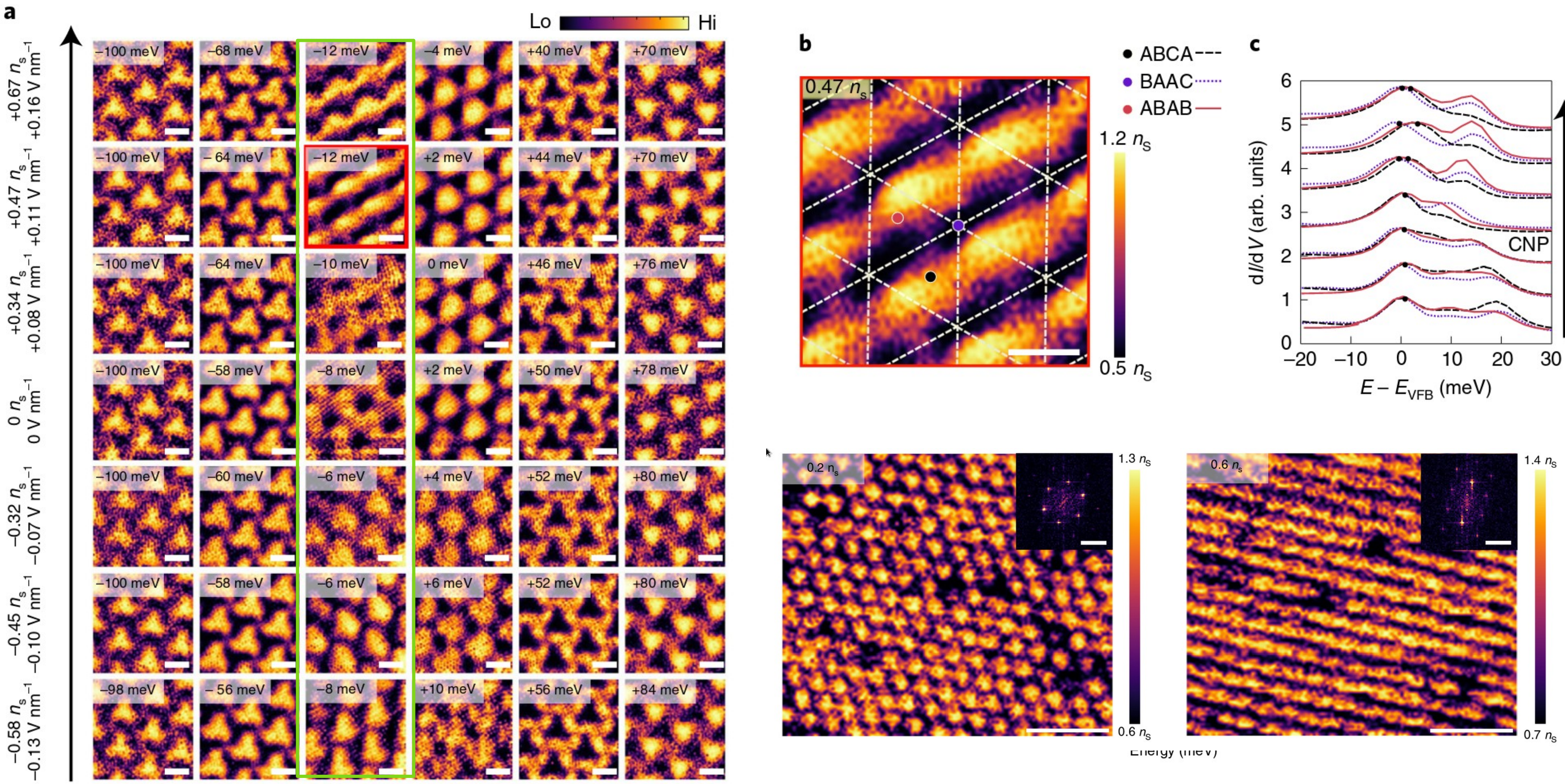

Nematicity in TDBG

spin, layer, sublattice and valley degrees of freedom

$$\mathcal{H}_{\mathbf{\Phi}} = \int_{\boldsymbol{r}} \int_{\Delta \boldsymbol{r}} \mathbf{\Phi} \cdot \phi_{\ell,s,\eta;\ell',s',\eta'}(\boldsymbol{r}, \Delta \boldsymbol{r})\, c^{\dagger}_{\sigma,\overbrace{\ell,s,\eta}}(\boldsymbol{r} + \Delta \boldsymbol{r}) c_{\sigma,\ell',s',\eta'}(\mathbf{r}) + \mathrm{H.c.}$$

intensity

$$\mathbf{\Phi} = \Phi\,(\cos 2\varphi, \sin 2\varphi)$$

nematic director angle

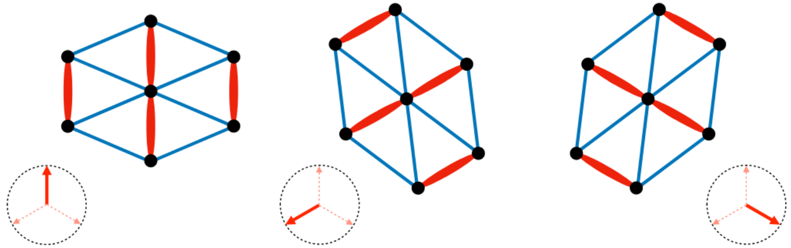

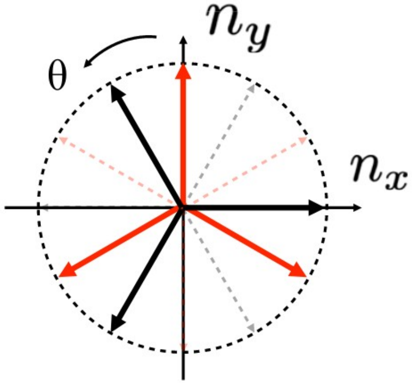

- Graphene nematicity (GN);
- Moiré Nematicity (MN);

R. Samajdar, M. S. Scheurer, S. Turkel, et al. 2D Materials 8, 034005 (2021).

Moiré Nematicity (MN)

$$\mathcal{H}_{\mathbf{\Phi}}^{MN} = \mathbf{\Phi} \cdot \boldsymbol{f}\left(\boldsymbol{k}\right) c_{\alpha}^{\dagger}\left(\boldsymbol{k}\right) c_{\alpha}\left(\boldsymbol{k}\right)$$

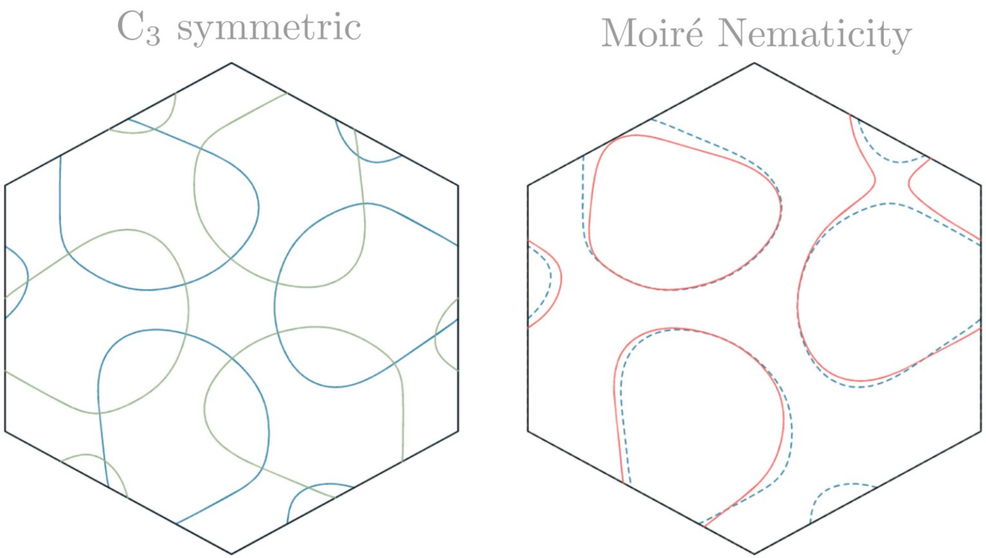

$$E_{n,\boldsymbol{k}} \to E_{n,\boldsymbol{k}} + \mathbf{\Phi} \cdot \boldsymbol{f}(\boldsymbol{k}),$$

$$\boldsymbol{f}(\boldsymbol{k}) = \sum_{m_1,m_2 \in \mathbb{Z}} \boldsymbol{\phi}_{m_1,m_2} \cos(\boldsymbol{k} \cdot \boldsymbol{R}_{m_1,m_2})$$

→ Transforms as E irred. of D_3

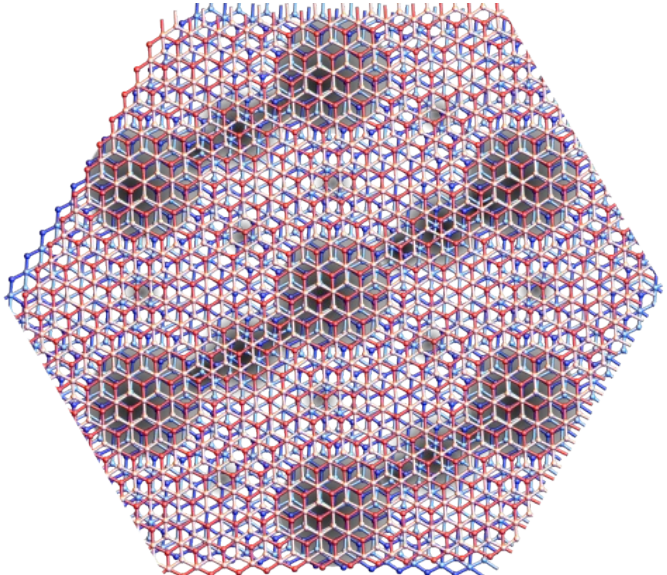

- Stronger effects close to van-Hove singularities
- Breaks C3 symmetry at moiré scale.
- Learnable parameters: φ_{MN} and Φ_{MN}.

Moiré Nematicity (MN)

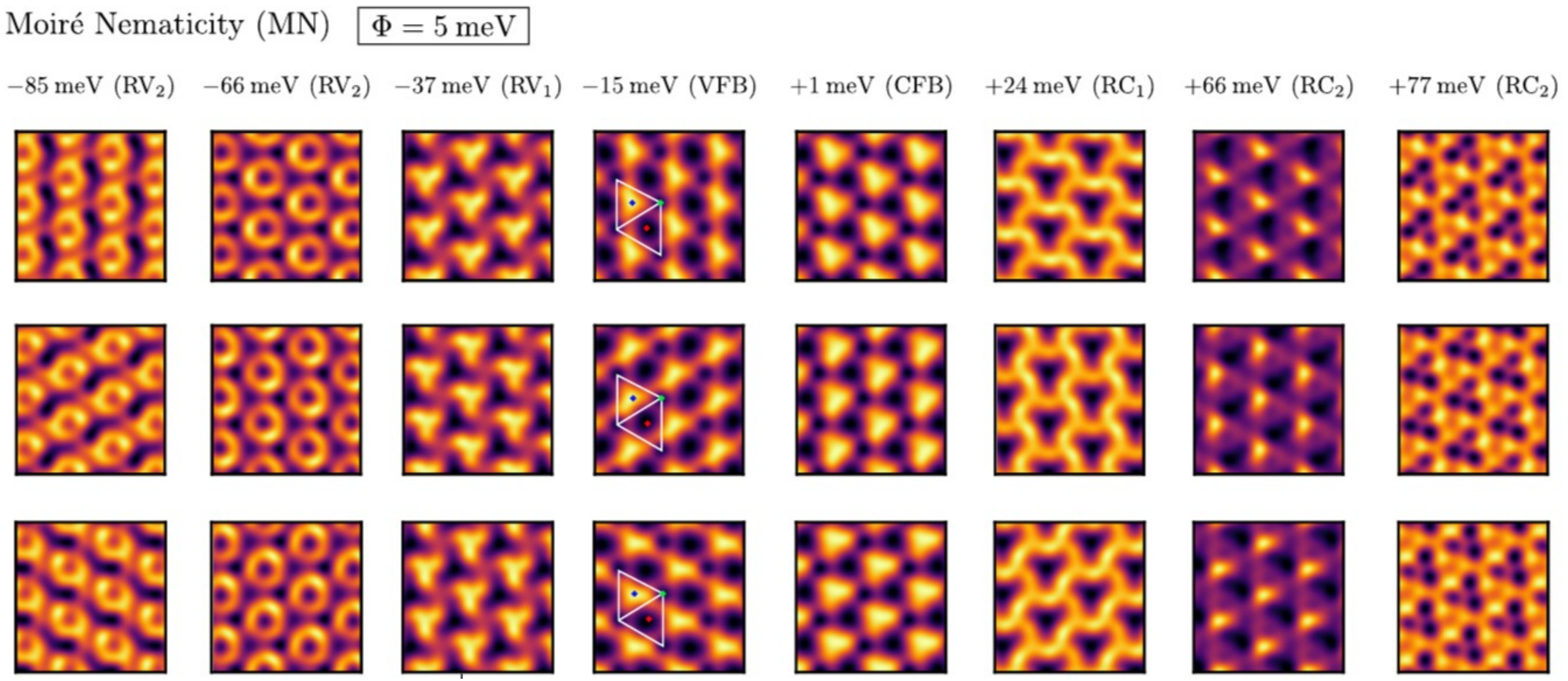

Graphene nematicity (GN)

$$\phi_{l,s;\,l',s'}\left(\eta\right) = \delta_{l,l'}\psi_l \begin{pmatrix} \left(e^{i\alpha_l \eta \rho_z}\rho_{\boldsymbol{x}}\right)_{ss'} \\ \eta\left(e^{i\alpha_l \eta \rho_z}\rho_y\right)_{ss'} \end{pmatrix}, \quad \psi_l, \alpha_l \in \mathbb{R}.$$

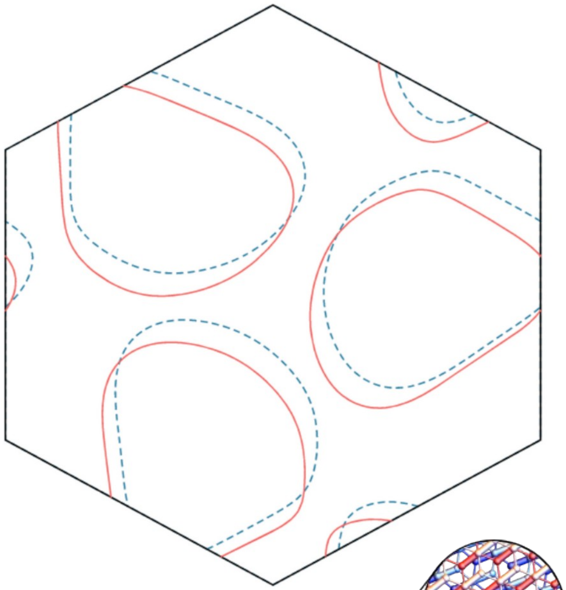

$$H_0\left(\boldsymbol{k}\right) \to H_0\left(\boldsymbol{k}\right) + \boldsymbol{\Phi}\cdot\boldsymbol{\phi}_{s,s'} =$$

$$= \begin{pmatrix} 0 & -\hbar\nu k_- + \boldsymbol{\Phi}\cdot M_\alpha \\ -\hbar\nu k_+ + \boldsymbol{\Phi}\cdot M_\alpha^\dagger & d \end{pmatrix} \quad M_{\alpha_l} = \left(1, -i\eta\right)e^{i\alpha_l\eta}.$$

$$\mathcal{H}_l = -\hbar\nu\left[R\left(\pm\theta/2\right)\left(\boldsymbol{k} - \boldsymbol{K}_\eta^l\right)\right]\cdot\left(\eta\rho_x, \rho_y\right) + \boxed{\boldsymbol{\Phi}\cdot\left(\rho_x, \eta\rho_y\right)}$$

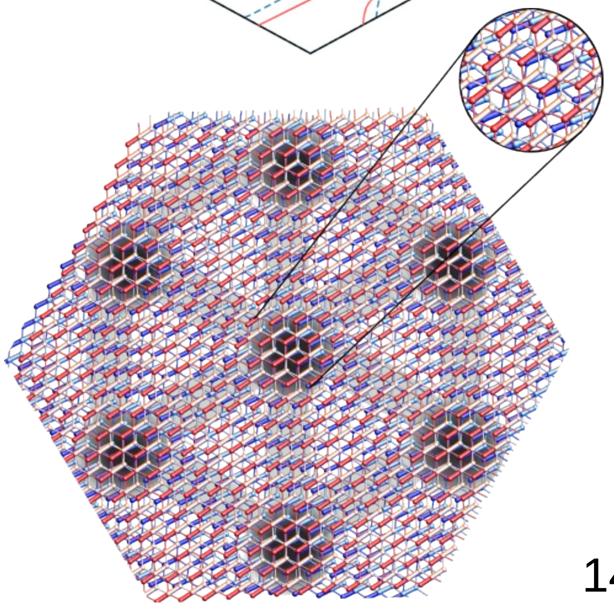

- Shifts Dirac cones.
- Breaks C3 symmetry at atomic scale;
- Learnable parameters: $\varphi_{GN}, \Phi_{GN}, \alpha, \ldots$

Graphene nematicity (GN)

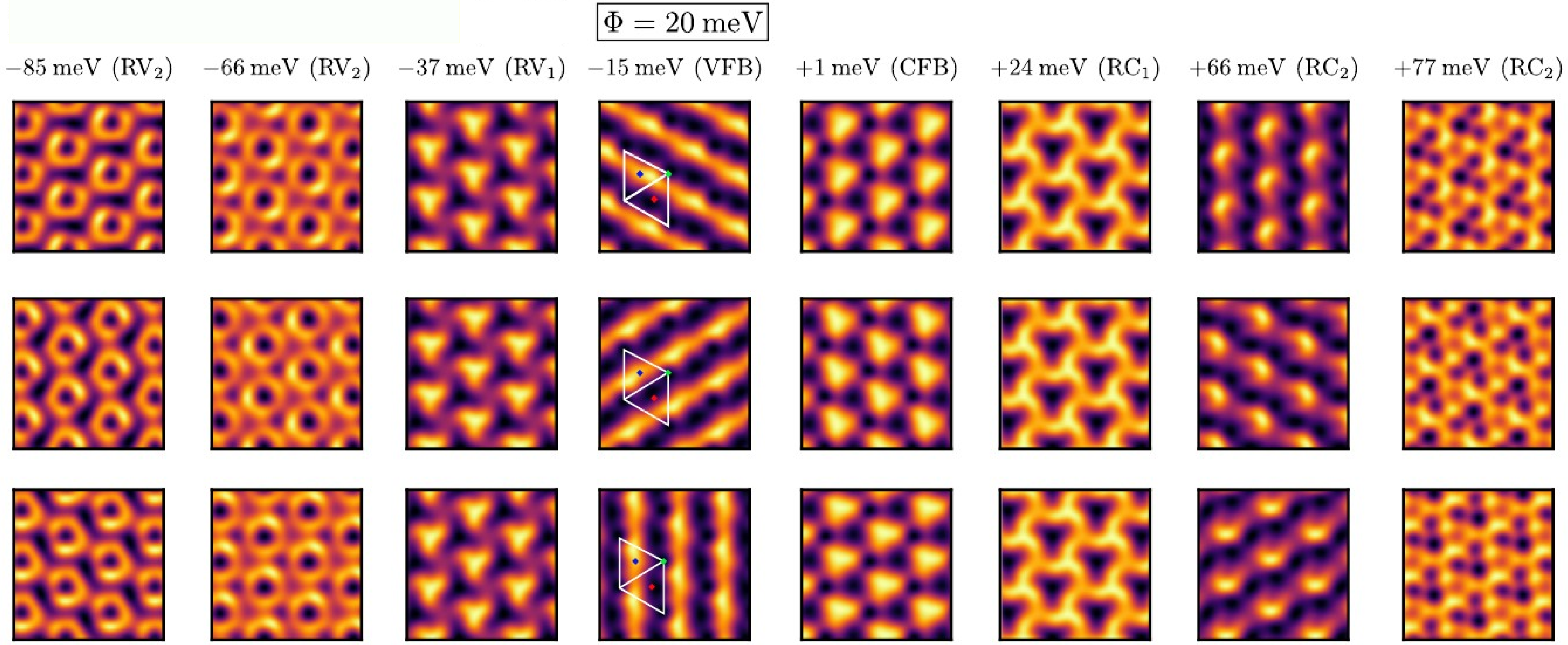

Solving the Inverse Problem

$$H_{\mathbf{k}} = H_{\mathbf{k}}\left[t_j\right]$$

↓ Symmetry breaking phenomena

$$H_{\mathbf{k}} \to H_{\mathbf{k}} + \phi_\mu g^{\mu}_{\mathbf{k}}[\{\beta\}]$$

$$\beta = F^{-1}_{H_{\mathbf{k}}}\left(\mathcal{O}\right)$$

$$\frac{\mathrm{dI}}{\mathrm{dV}}\left(\mathbf{r}, V\right)$$

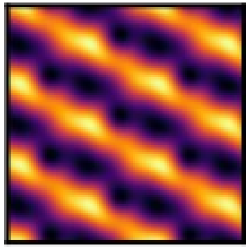

$$\mathcal{O} = F_{H_{\mathbf{k}}}\left(\beta\right) = \left\{\mathcal{D}\left(\mathbf{r}, \omega\right)\right\}_{\beta}$$

Microscopic parameters

DL Architecture

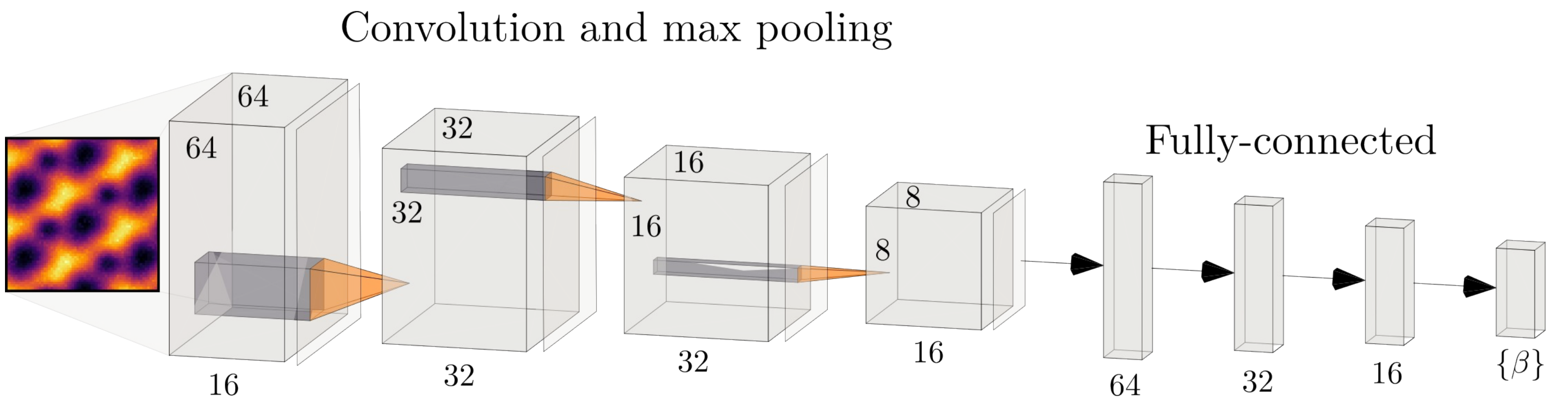

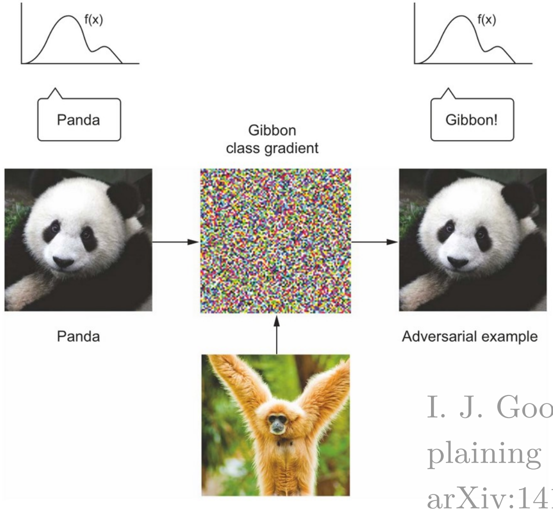

$$p_g\left(z\right) = \frac{\exp(-(z-\mu)^2/2\sigma^2)}{\sqrt{2\pi\sigma^2}}$$

$$\sigma \approx 0.31, \mu = 0$$

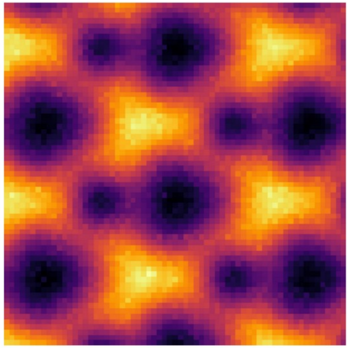

I. J. Goodfellow, J. Shlens, and C. Szegedy, "Explaining and Harnessing Adversarial Examples," (2015), arXiv:1412.6572 [cs, stat].

CNN's learning procedure

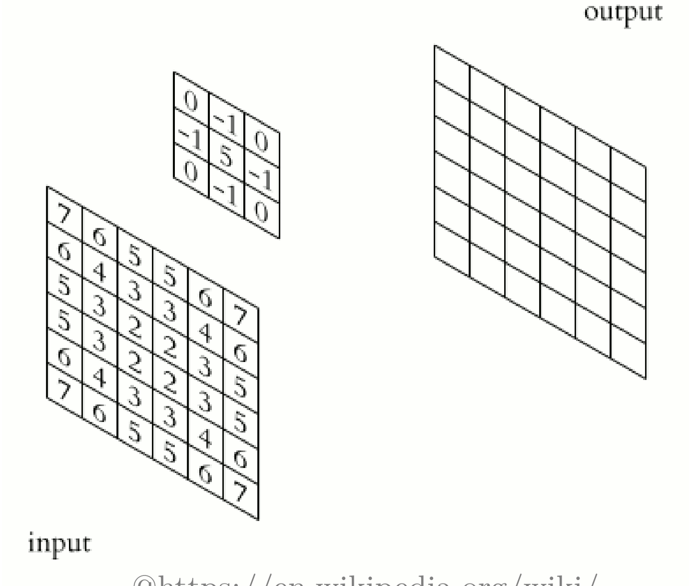

@https://en.wikipedia.org/wiki/Kernel_(image_processing)

Operation	Kernel ω	Image result g(x,y)
Identity	$\begin{bmatrix} 0 & 0 & 0 \\ 0 & 1 & 0 \\ 0 & 0 & 0 \end{bmatrix}$	
Ridge detection	$\begin{bmatrix} -1 & -1 & -1 \\ -1 & 4 & -1 \\ -1 & -1 & -1 \end{bmatrix}$	
	$\begin{bmatrix} -1 & -1 & -1 \\ -1 & 8 & -1 \\ -1 & -1 & -1 \end{bmatrix}$	

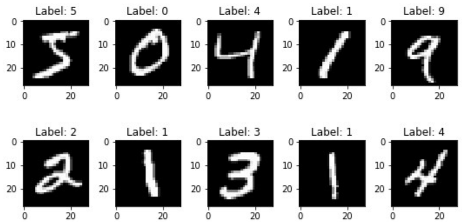

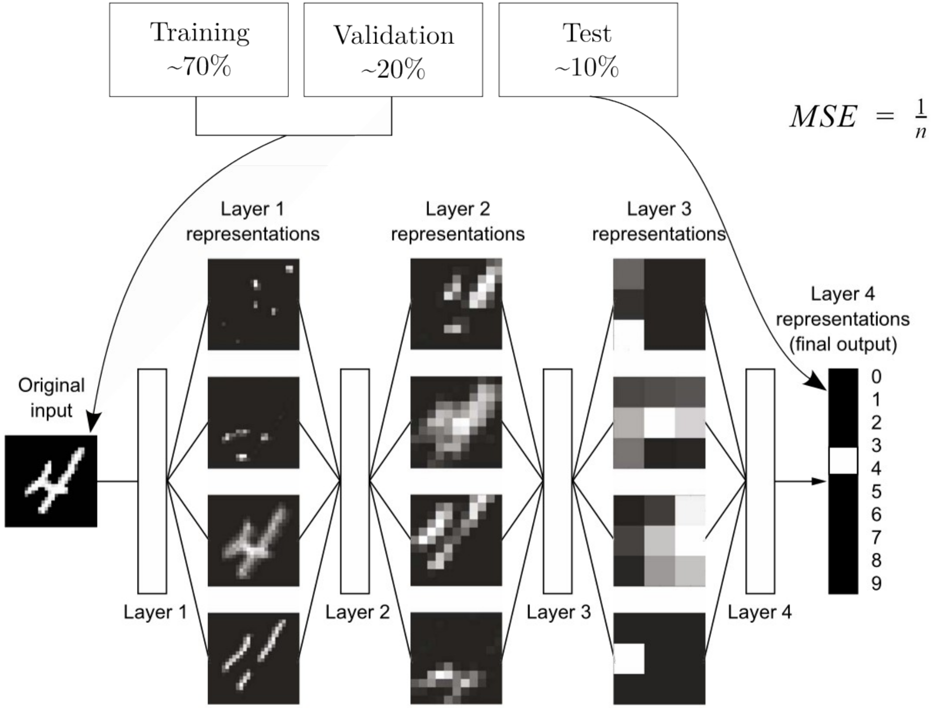

$$MSE = \frac{1}{n} \Sigma \underbrace{\left(y - \widehat{y} \right)^2}_{\text{The square of the difference between actual and predicted}}$$

DL Architecture

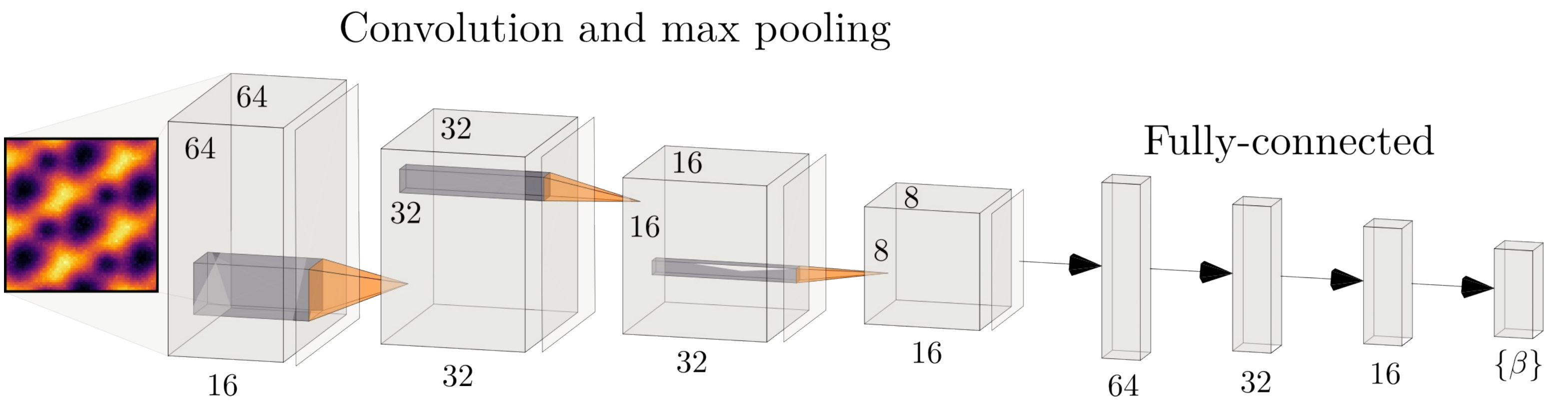

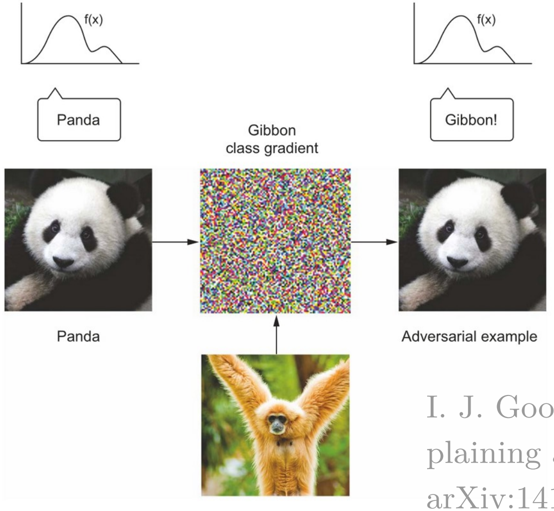

$$p_g\left(z\right) = \frac{\exp(-(z-\mu)^2/2\sigma^2)}{\sqrt{2\pi\sigma^2}}$$

$$\sigma \approx 0.31, \mu = 0$$

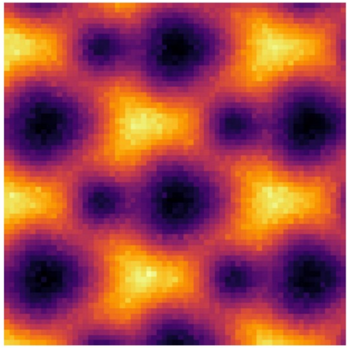

I. J. Goodfellow, J. Shlens, and C. Szegedy, "Explaining and Harnessing Adversarial Examples," (2015), arXiv:1412.6572 [cs, stat].

Orientation of Nematic Director

intensity

$$\mathbf{\Phi} = \Phi\left(\cos 2\varphi, \sin 2\varphi\right)$$

nematic director angle

$$\varphi_i = \frac{1}{2}\mathrm{arctan2}\left(\sin 2\varphi, \cos 2\varphi\right) \Rightarrow$$

$$\Rightarrow \varphi = \begin{cases} \varphi_i, & \mathrm{sgn}\varphi_i = 1 \\ \varphi_i + \pi, & \mathrm{sgn}\varphi_i = -1 \end{cases}$$

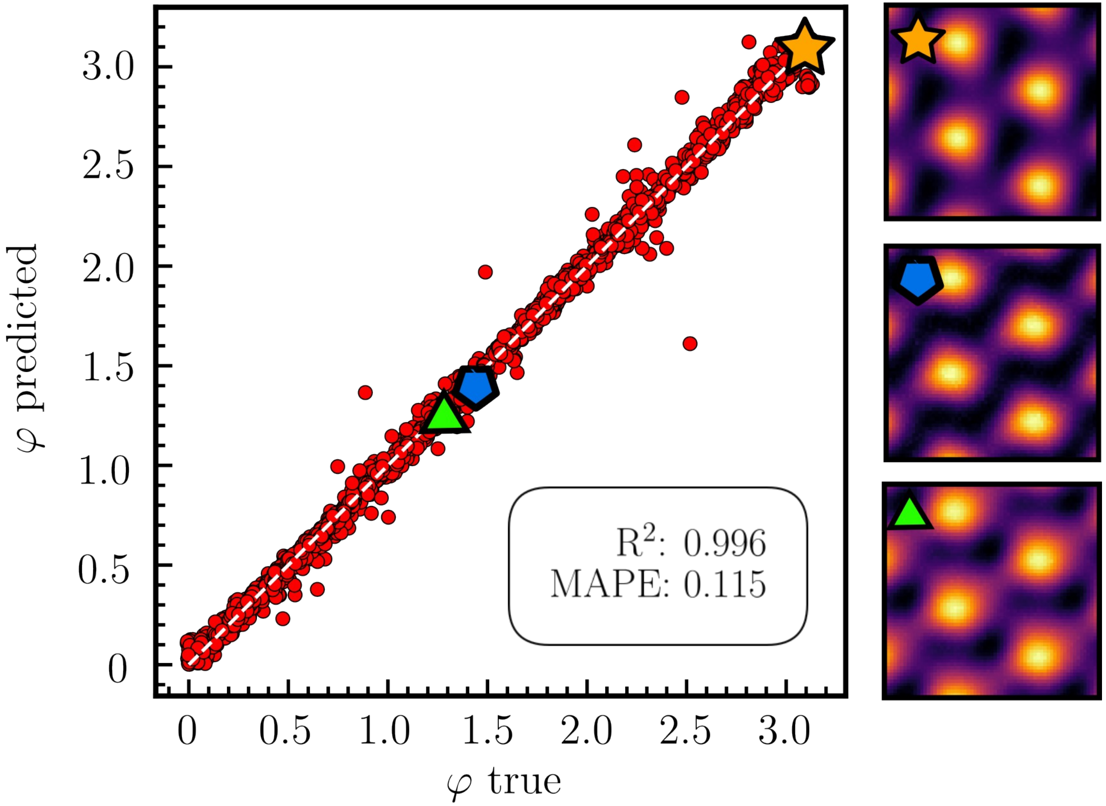

$$\mathcal{D}_{\mathrm{th}} \rightarrow \phi_{\mathrm{MN}}, \phi_{\mathrm{GN}} \in [0.001, 0.1]\ \mathrm{eV}, \varphi = \varphi_{\mathrm{MN}} = \varphi_{\mathrm{GN}} \in [0, \pi]$$

More data: Adding $\mathcal{D}_{\mathbf{r}_0}(\omega)$ channels

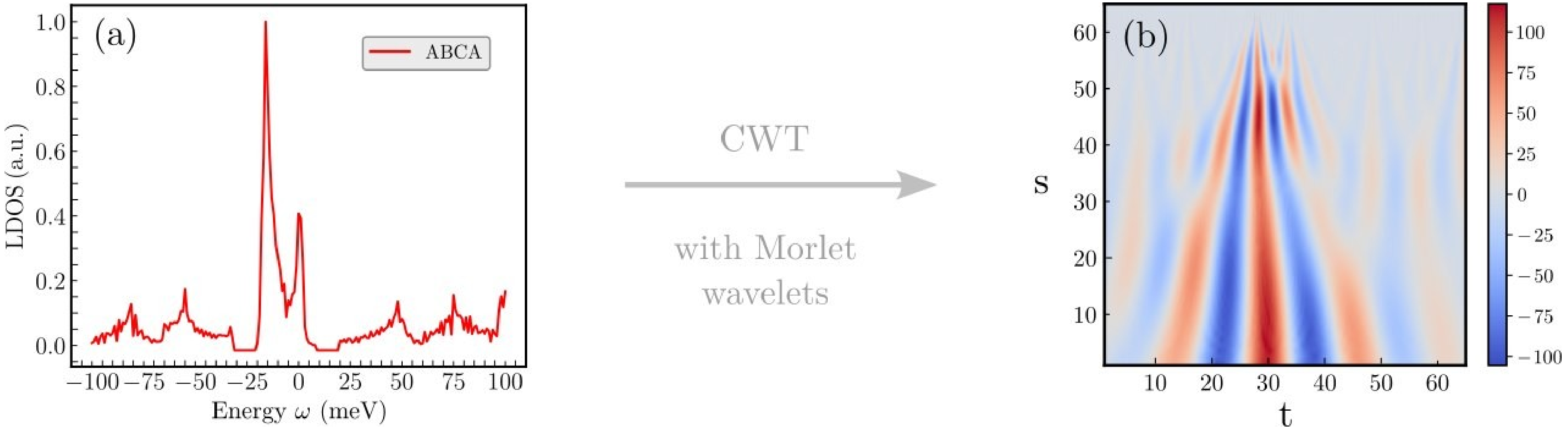

with gaussian noise $$p_G(z) = \frac{1}{\sigma\sqrt{2\pi}} e^{-\frac{(z-\mu)^2}{2\sigma^2}}$$ $\sigma = 0.31, \mu = \mathcal{D}(\omega)$

New architecture

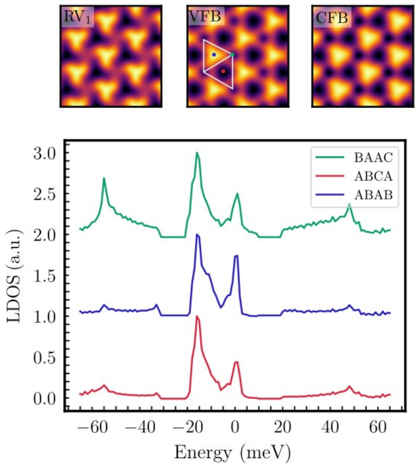

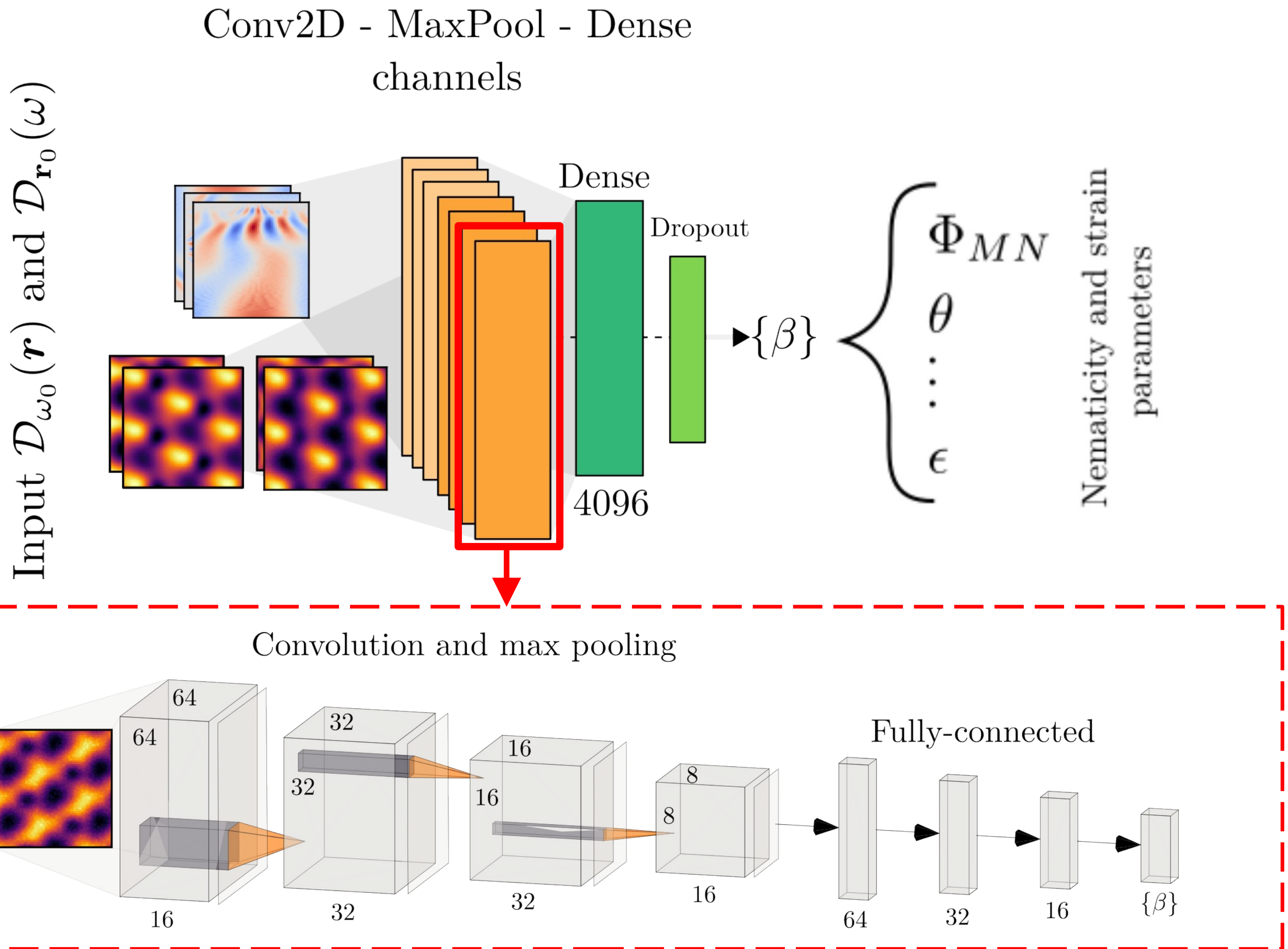

Back to the nematic microscopic form

$$E_{n,\boldsymbol{k}} \to E_{n,\boldsymbol{k}} + \boldsymbol{\Phi} \cdot \boldsymbol{f}(\boldsymbol{k}),$$

$$\boldsymbol{f}(\boldsymbol{k}) = \sum_{m_1, m_2 \in \mathbb{Z}} \boldsymbol{\phi}_{m_1,m_2} \cos(\boldsymbol{k} \cdot \boldsymbol{R}_{m_1,m_2})$$

$$H_0(\boldsymbol{k}) \to H_0(\boldsymbol{k}) + \boldsymbol{\Phi} \cdot \boldsymbol{\phi}_{s,s'} = \begin{pmatrix} 0 & -\hbar\nu k_- + \boldsymbol{\Phi} \cdot M_\alpha \\ -\hbar\nu k_+ + \boldsymbol{\Phi} \cdot M_\alpha^\dagger & d \end{pmatrix}$$

$$M_{\alpha_l} = (1, -i\eta)\, e^{i\alpha_l \eta}.$$

Learn $\beta = \{\Phi_{\mathrm{MN}}, \Phi_{\mathrm{GN}}, \alpha\}$

Form of nematicity

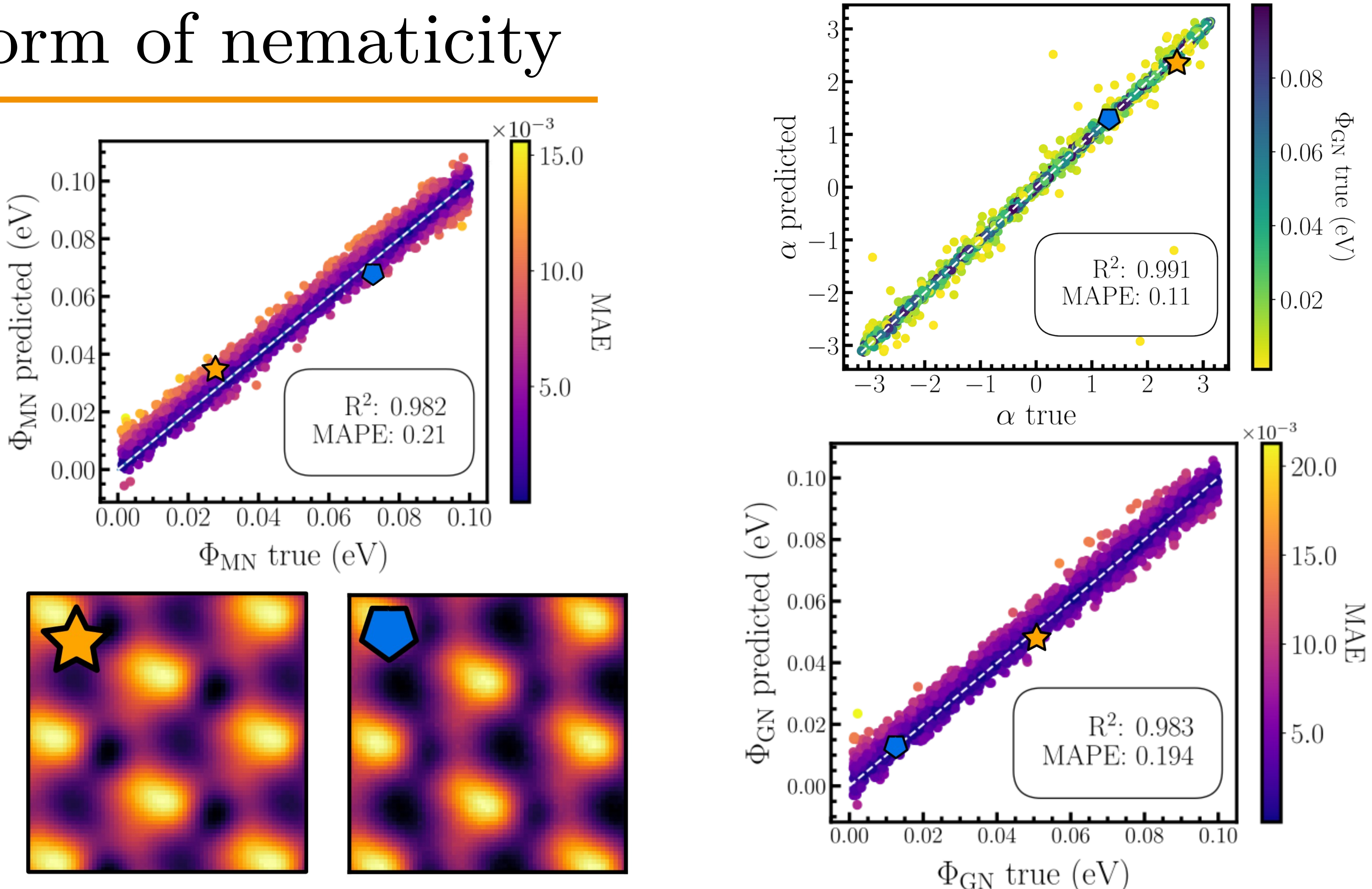

Including strain

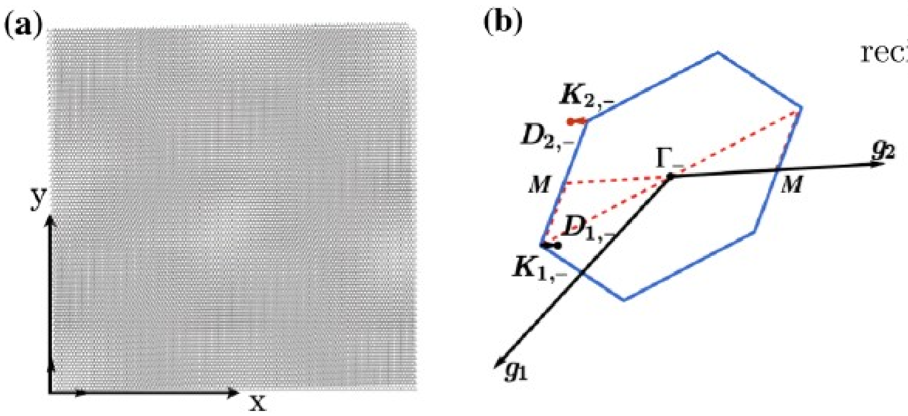

Fig. 1: Modification of Moiré Structure and Brillouin Zone with $\epsilon = 0.7\%, \varphi = 0^\circ$ *and* $\theta = 1.05^\circ$ [5].

moiré superlattice reciprocal and primitive latticevectors

$$\begin{cases} \mathbf{g}_i \cong \mathcal{E}^T \mathbf{G}_i \\ \mathbf{a}_i \cong \mathcal{E}^{-1} \mathbf{A}_i \end{cases}$$

monolayer graphene reciprocal and primitive latticevectors

small angle rotation

learnable parameters

$$\mathcal{E} = \mathcal{T}(\theta) + S_{ua}\left(\varepsilon, \theta_\varepsilon\right)$$

$$\mathcal{E} = \frac{1}{2} R(\theta_\epsilon)^{-1} \begin{pmatrix} -\epsilon & 0 \\ 0 & \nu\epsilon \end{pmatrix} R(\theta_\epsilon)$$

uniaxial strain

Bi, Z., Yuan, N.F. and Fu, L., 2019. Physical Review B, 100(3), p.035448.

Learn $\Phi_{\mathrm{MN}}, \Phi_{\mathrm{GN}}, \theta_\varepsilon, \epsilon$

Including strain

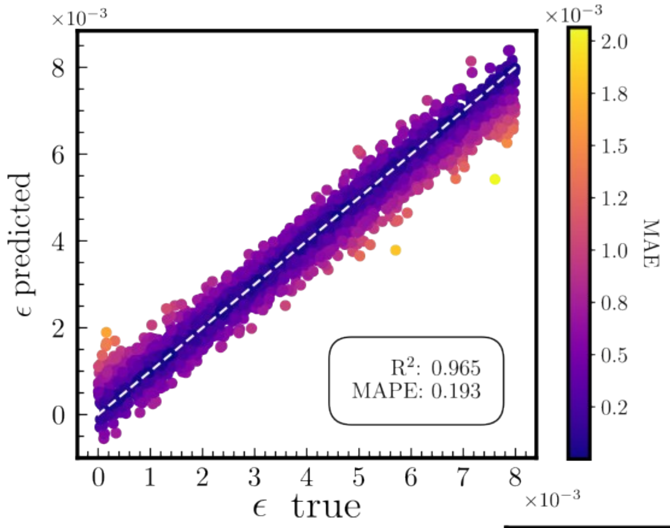

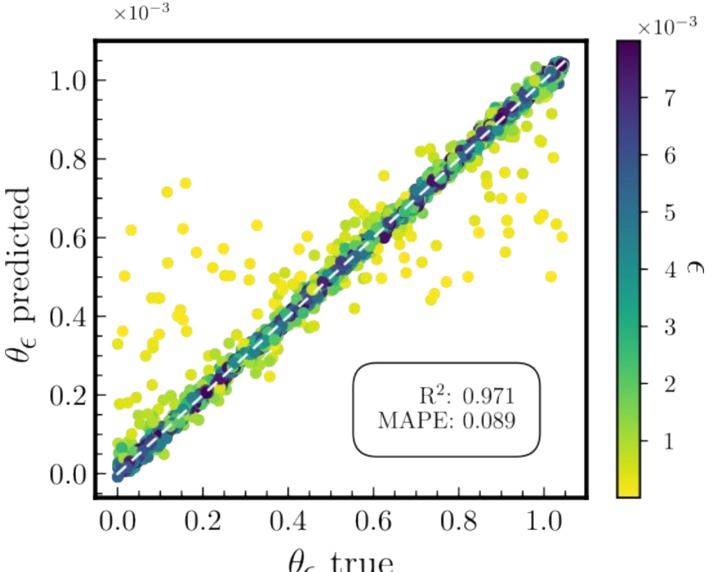

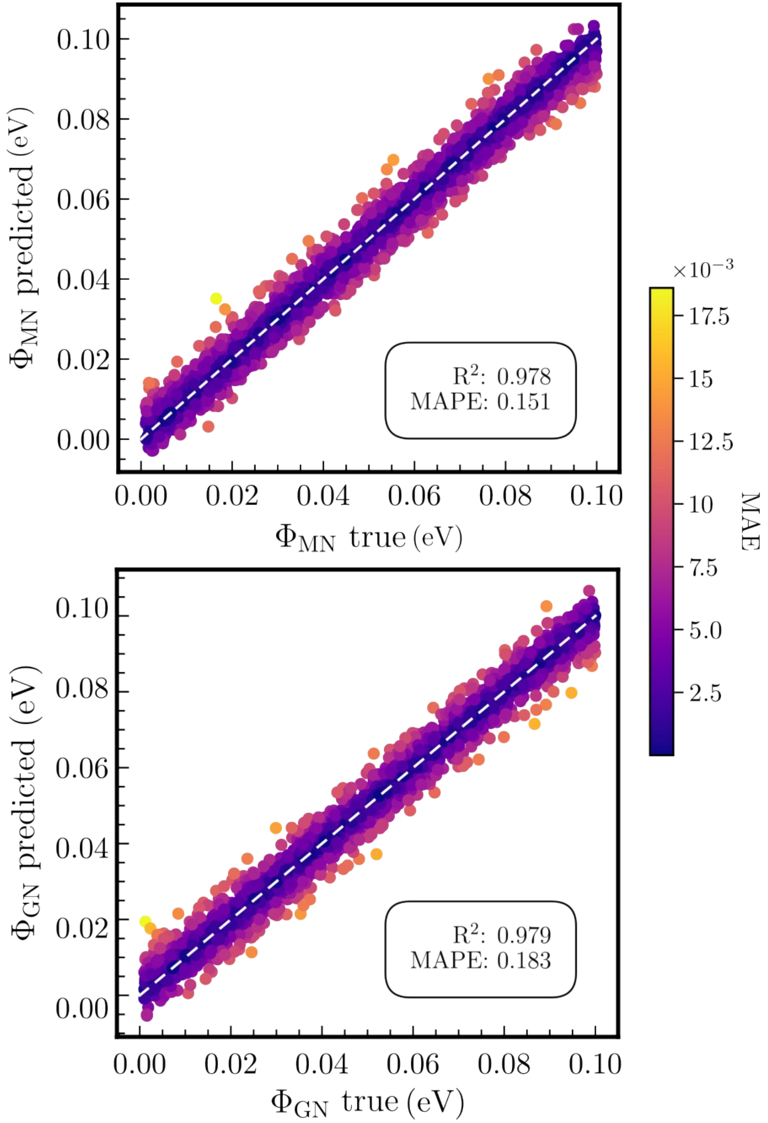

Including strain, fixed θ_ε

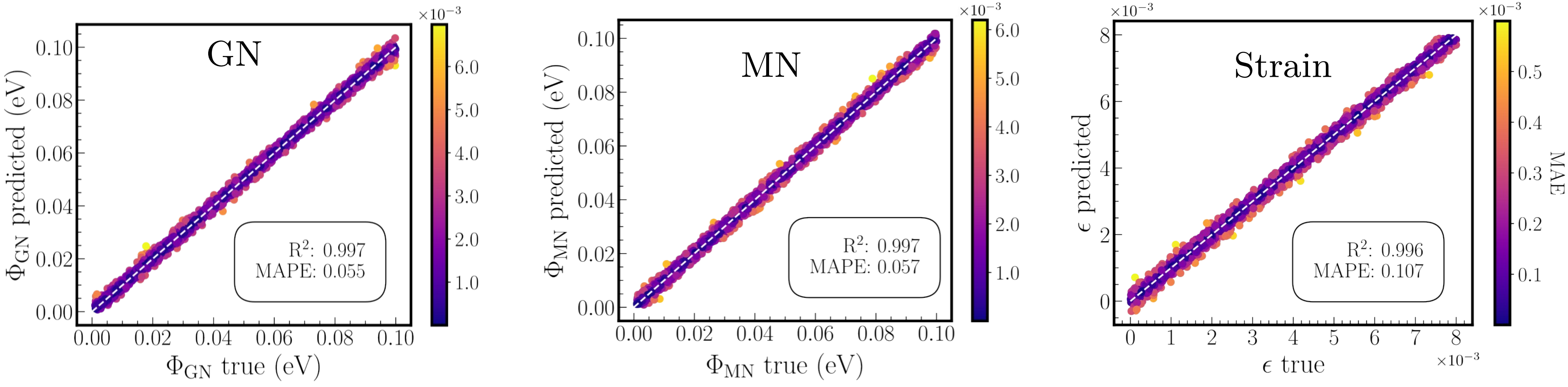

- Can we apply the trained CNN directly to experimental data?

Preprocessing of D_{exp}

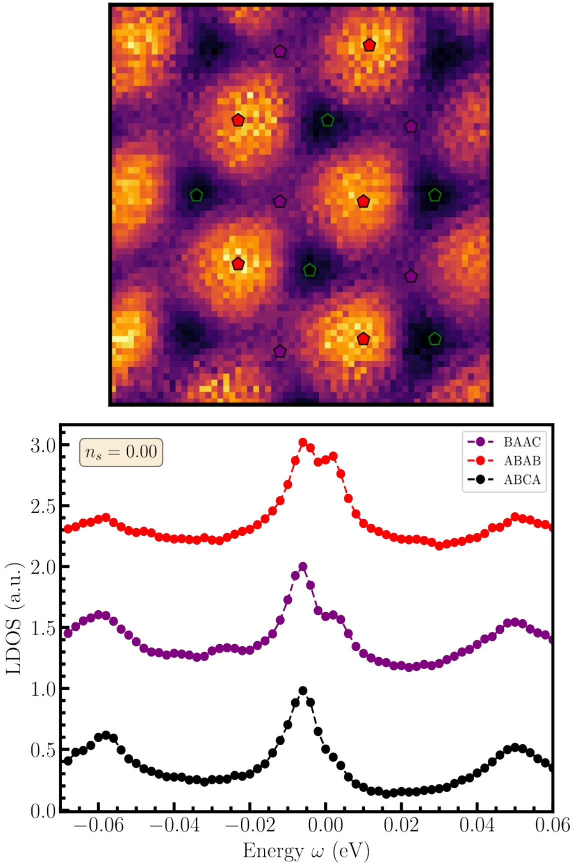

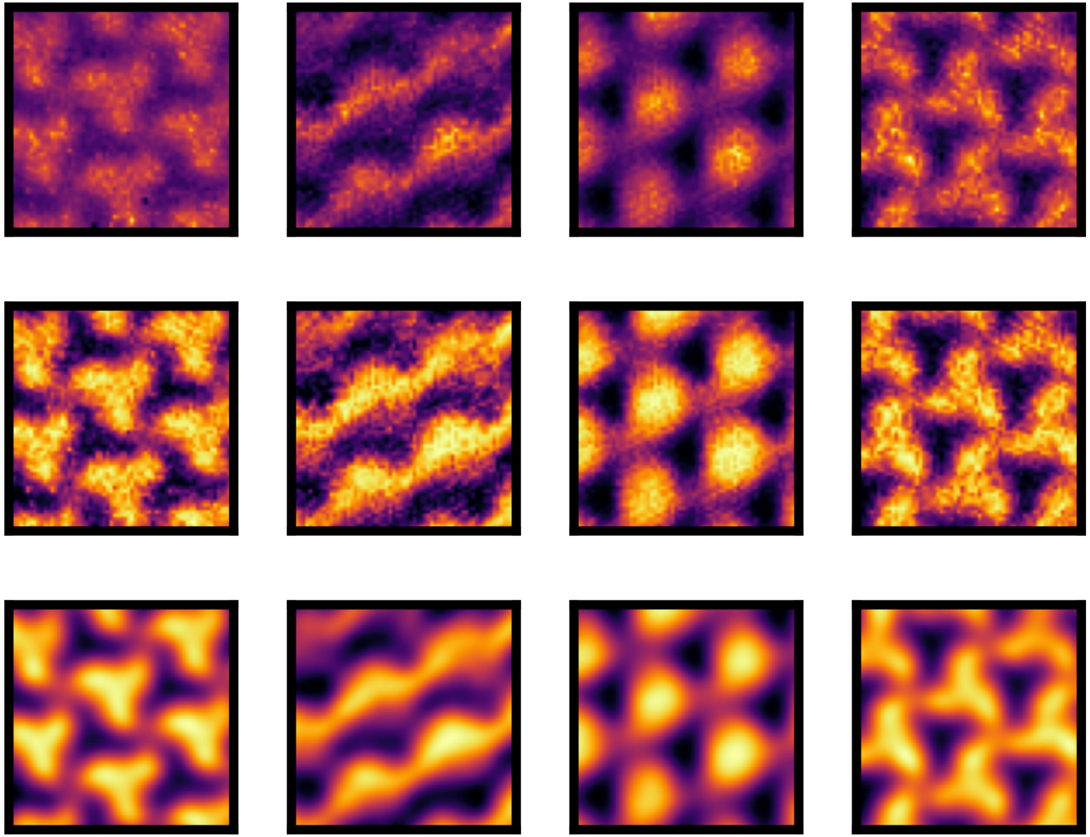

Predictions on D_{exp}

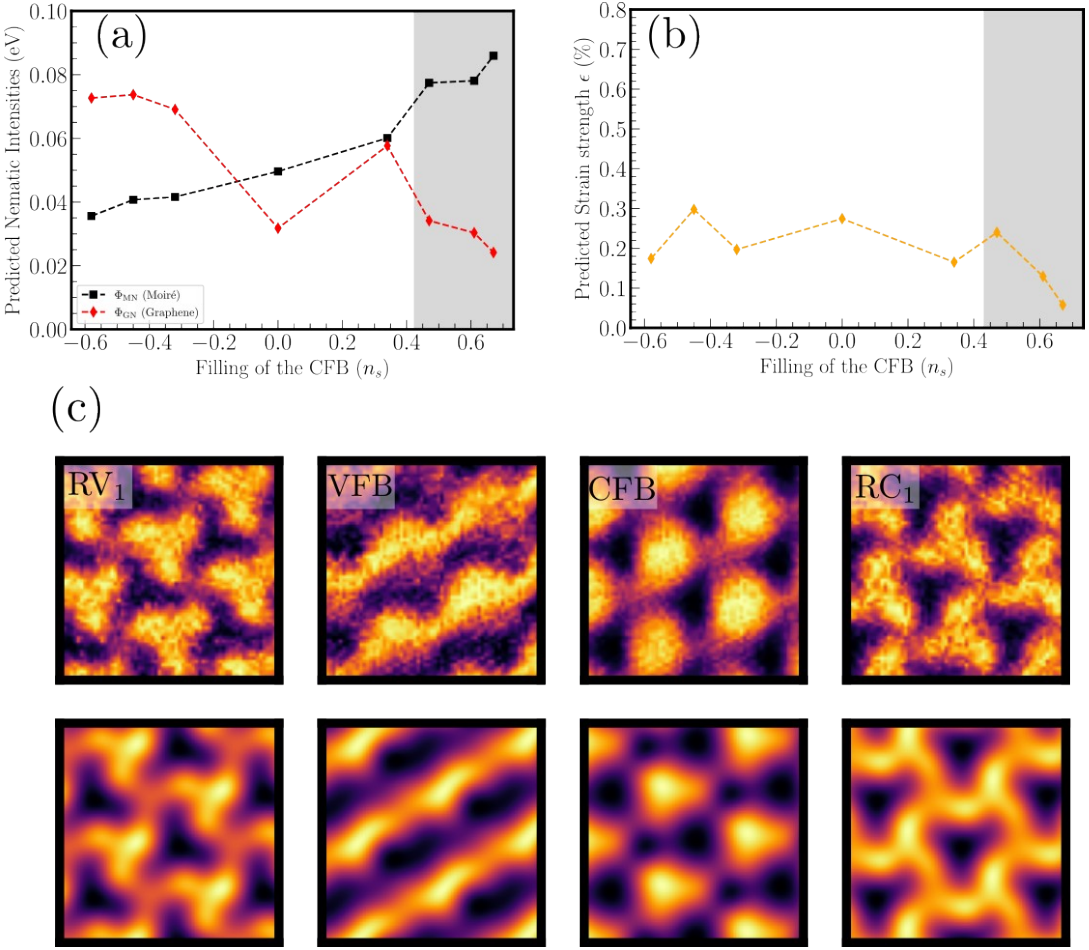

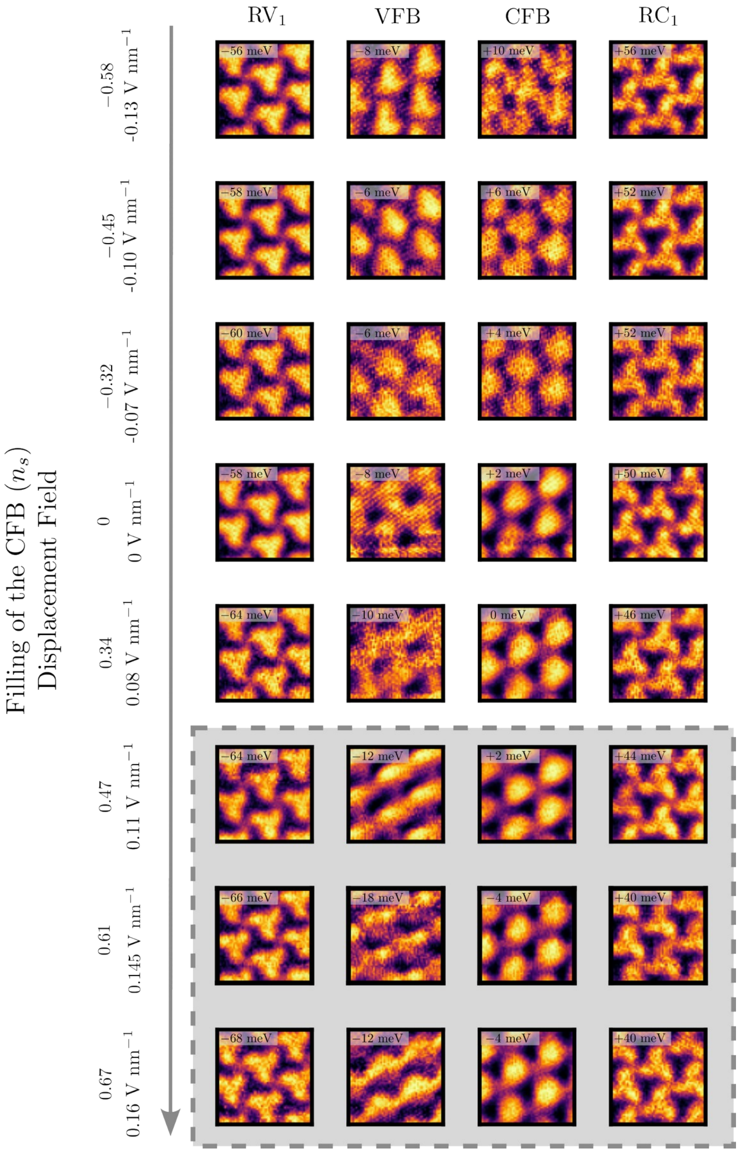

Prediction on D_{exp}(Preprocessing stage)

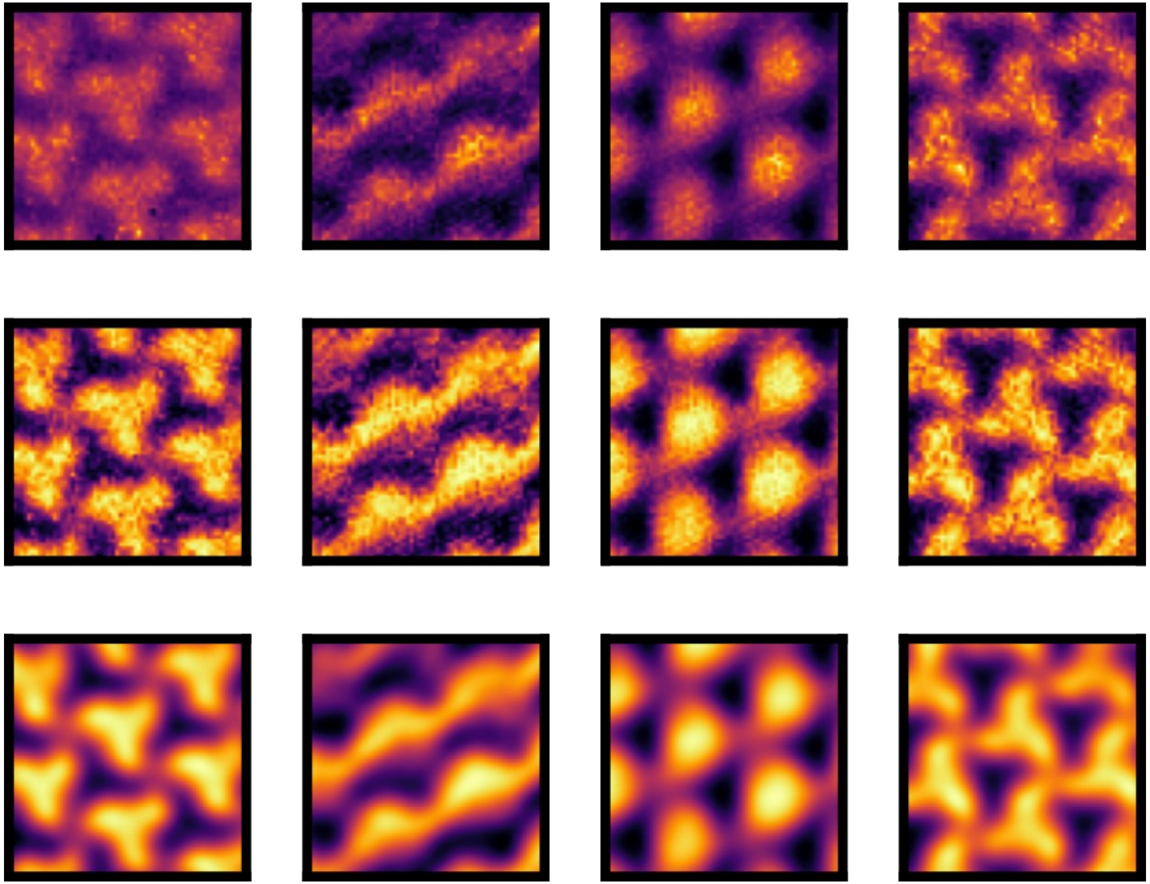

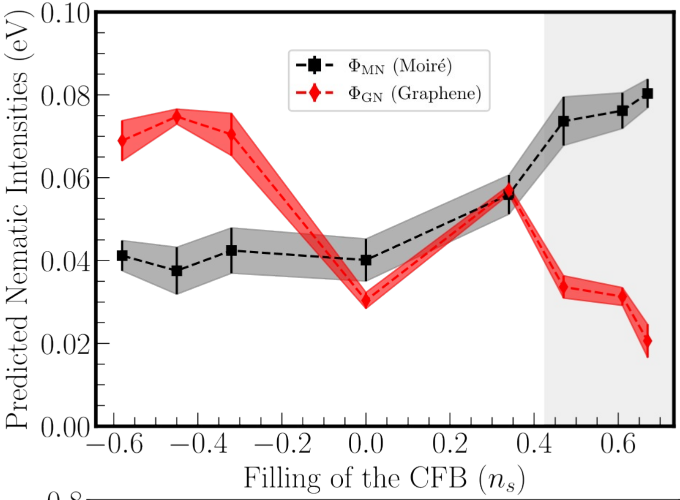

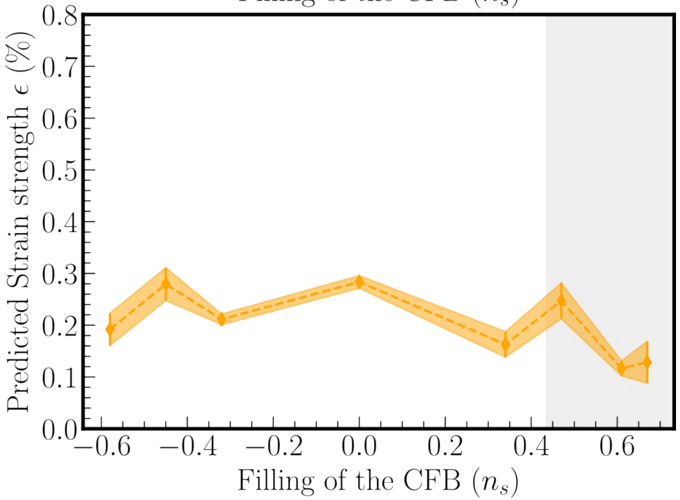

Beyond TDBG and the continuum model

Minimal tight-binding model

(four bands per spin &valley)

$$H = \sum_{\vec{k}} \sum_{l=1,2,} c^{\dagger}_{\vec{k},l}\, \vec{g}^{\,l}_{\vec{k}} \cdot \vec{\rho}\, c^{\dagger}_{\vec{k},l} + w_1 \sum_{\vec{k}} \left(e^{-i\theta_w} c^{\dagger}_{\vec{k},1} c_{\vec{k},2} + \text{H.c.} \right),$$

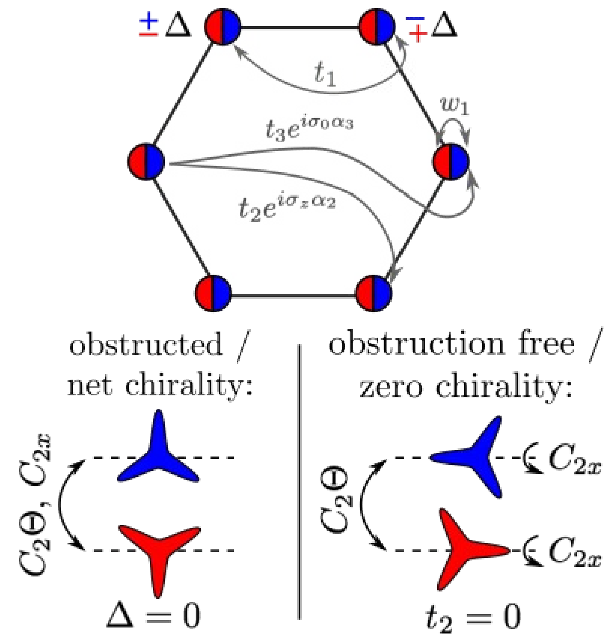

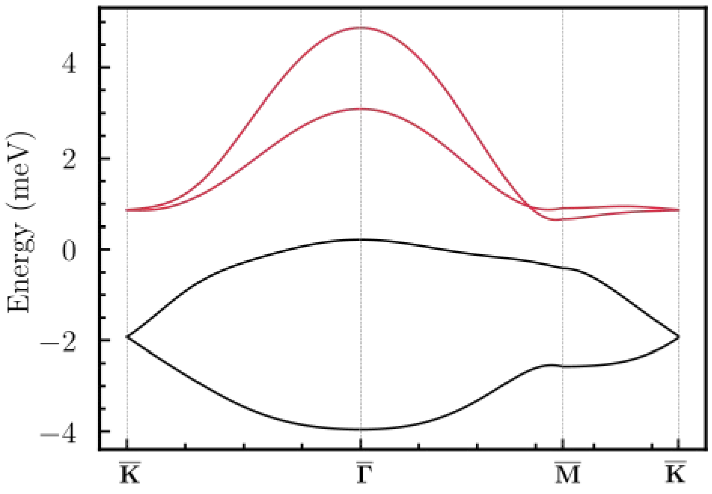

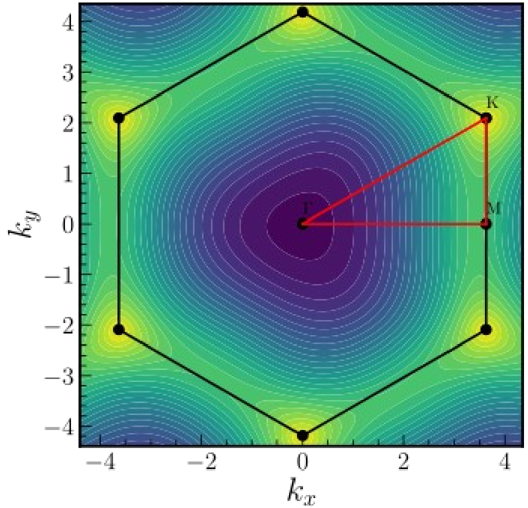

Beyond TDBG and the continuum model

Nematic order

$$\Delta h_{\boldsymbol{k}} = \boldsymbol{\phi} \cdot \boldsymbol{g}_{\boldsymbol{k}} = \phi_1 g_{1,\boldsymbol{k}} + \phi_2 g_{2,\boldsymbol{k}}$$

$$\boldsymbol{g}_{\boldsymbol{k}} \equiv \begin{pmatrix} g_{1,\boldsymbol{k}} \\ g_{2,\boldsymbol{k}} \end{pmatrix} = \alpha_0 \rho_0 \sigma_0 \begin{pmatrix} f_{1,\boldsymbol{k}} \\ f_{2,\boldsymbol{k}} \end{pmatrix} + \alpha_1 \rho_0 \sigma_x \begin{pmatrix} f_{1,\boldsymbol{k}} \\ f_{2,\boldsymbol{k}} \end{pmatrix} + \alpha_2 \rho_0 \sigma_y \begin{pmatrix} -f_{2,\boldsymbol{k}} \\ f_{1,\boldsymbol{k}} \end{pmatrix} + \alpha_3 \rho_z \sigma_z \begin{pmatrix} -f_{2,\boldsymbol{k}} \\ f_{1,\boldsymbol{k}} \end{pmatrix}$$

Learn $\alpha_0, \alpha_1, \alpha_2, \alpha_3$

if we focus on leading lattice harmonic

$$\boldsymbol{f}_{\boldsymbol{k}} = \frac{8}{3}\left(\cos k_y - \cos\frac{\sqrt{3}k_x}{2}\cos\frac{k_y}{2}, \sqrt{3}\sin\frac{\sqrt{3}k_x}{2}\sin\frac{k_y}{2}\right)^{\mathrm{T}}$$

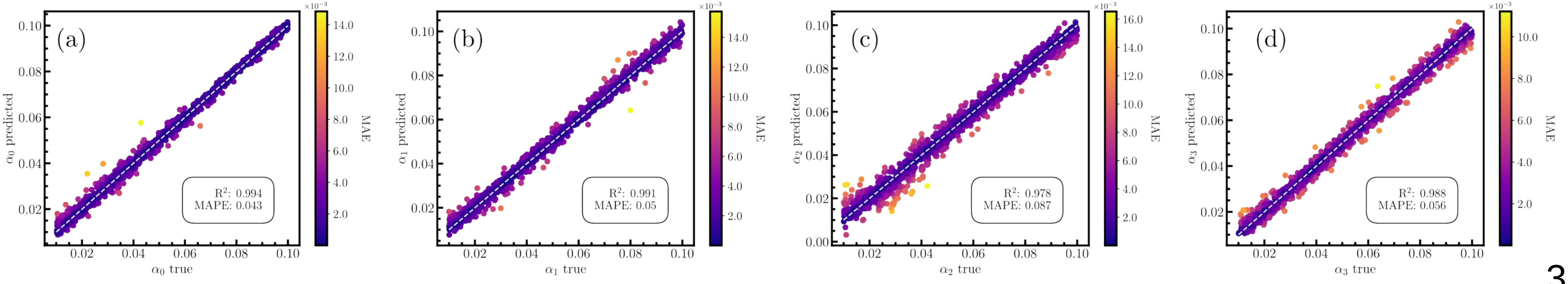

Overview and Outlook

- CNN’s can distinguish nematicity and strain influence.
- Possible crossover between GN and MN for TDBG;
- Applicability beyond the continuum model and TDBG;

- Microscopic parameter learning from data (kind of Hamiltonian Learning);
    - Automated analysis of larger datasets;
    - Extensible to a variety of experimental setups? Comparison between different theoretical models?

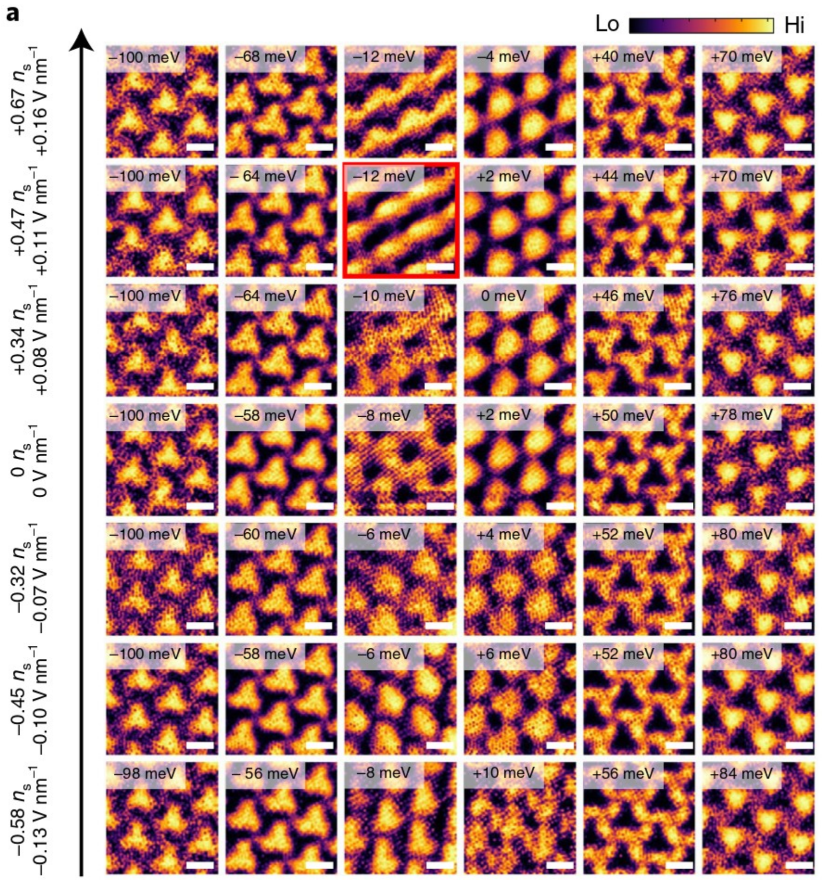

Backup slides

Number of channels and overfitting

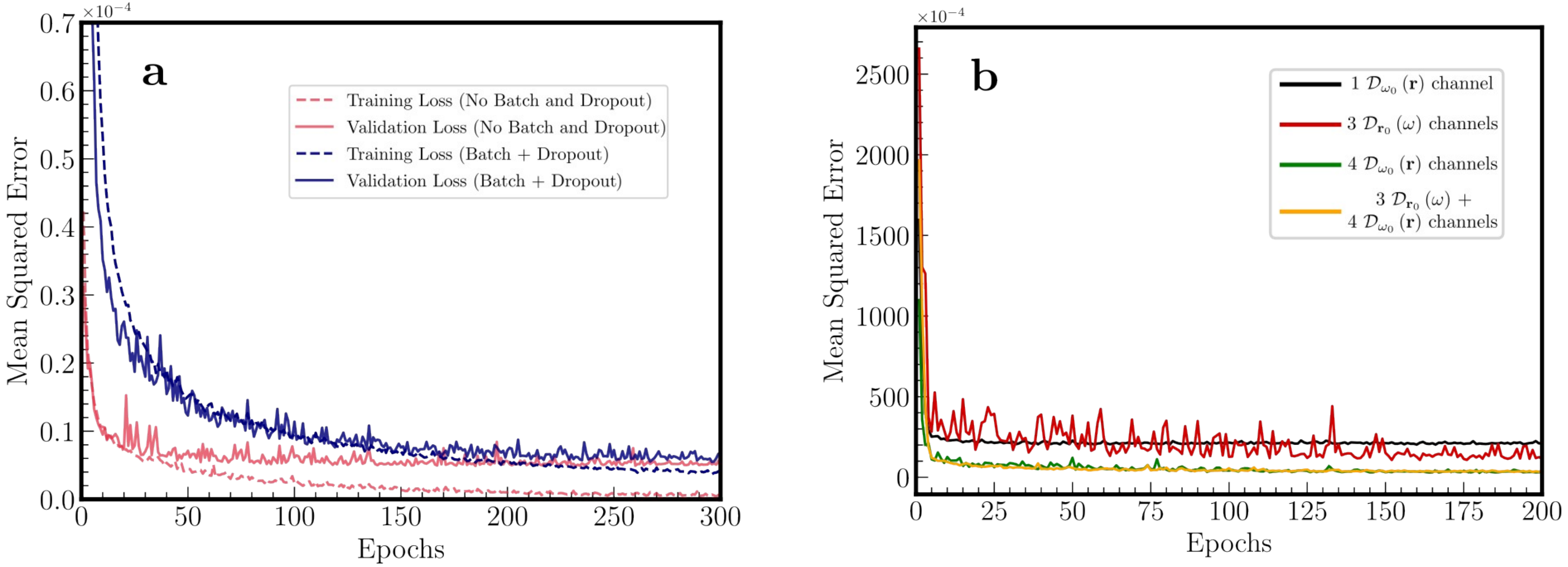

Average over different runs

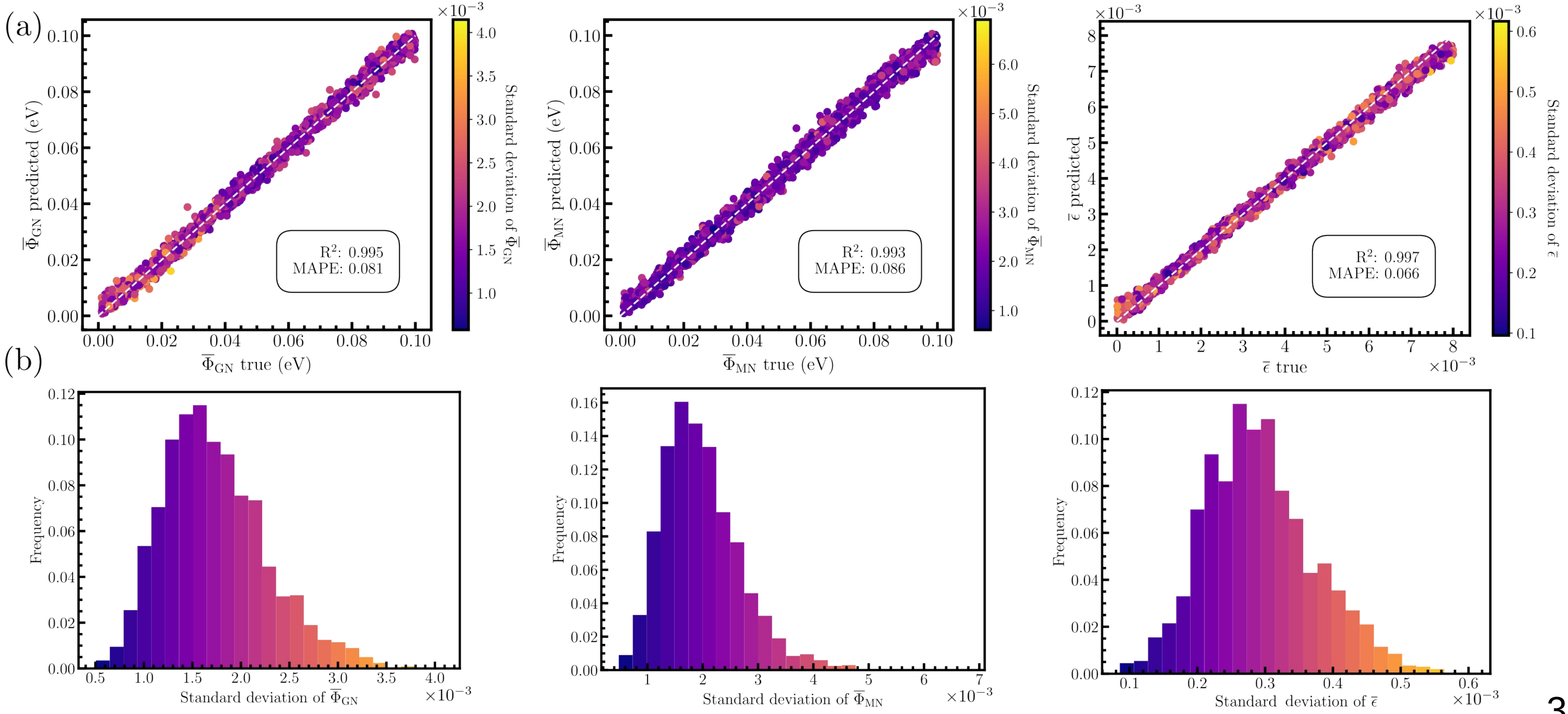

Robustness regarding impurities

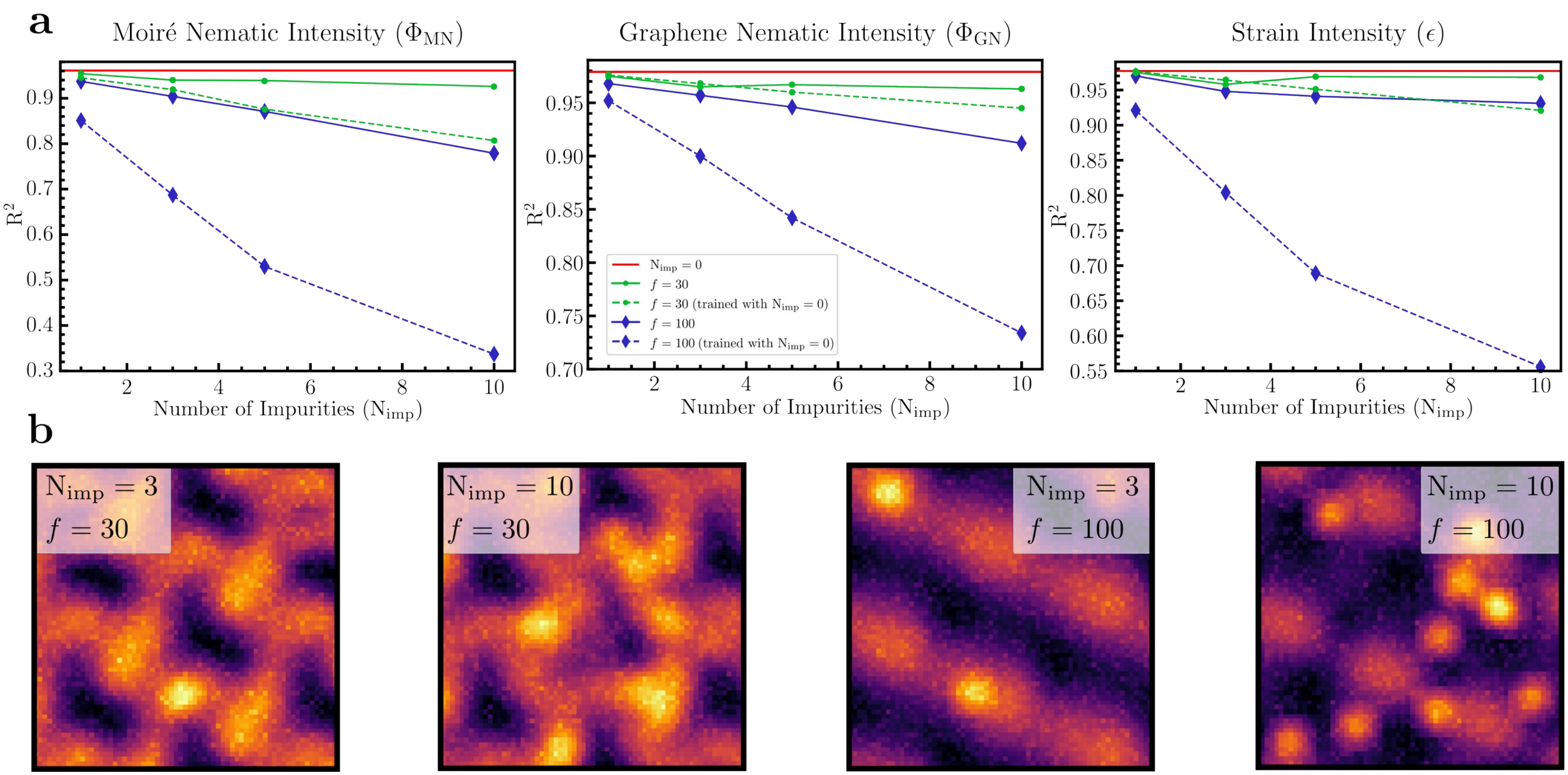

Preprocessing of the experimental data

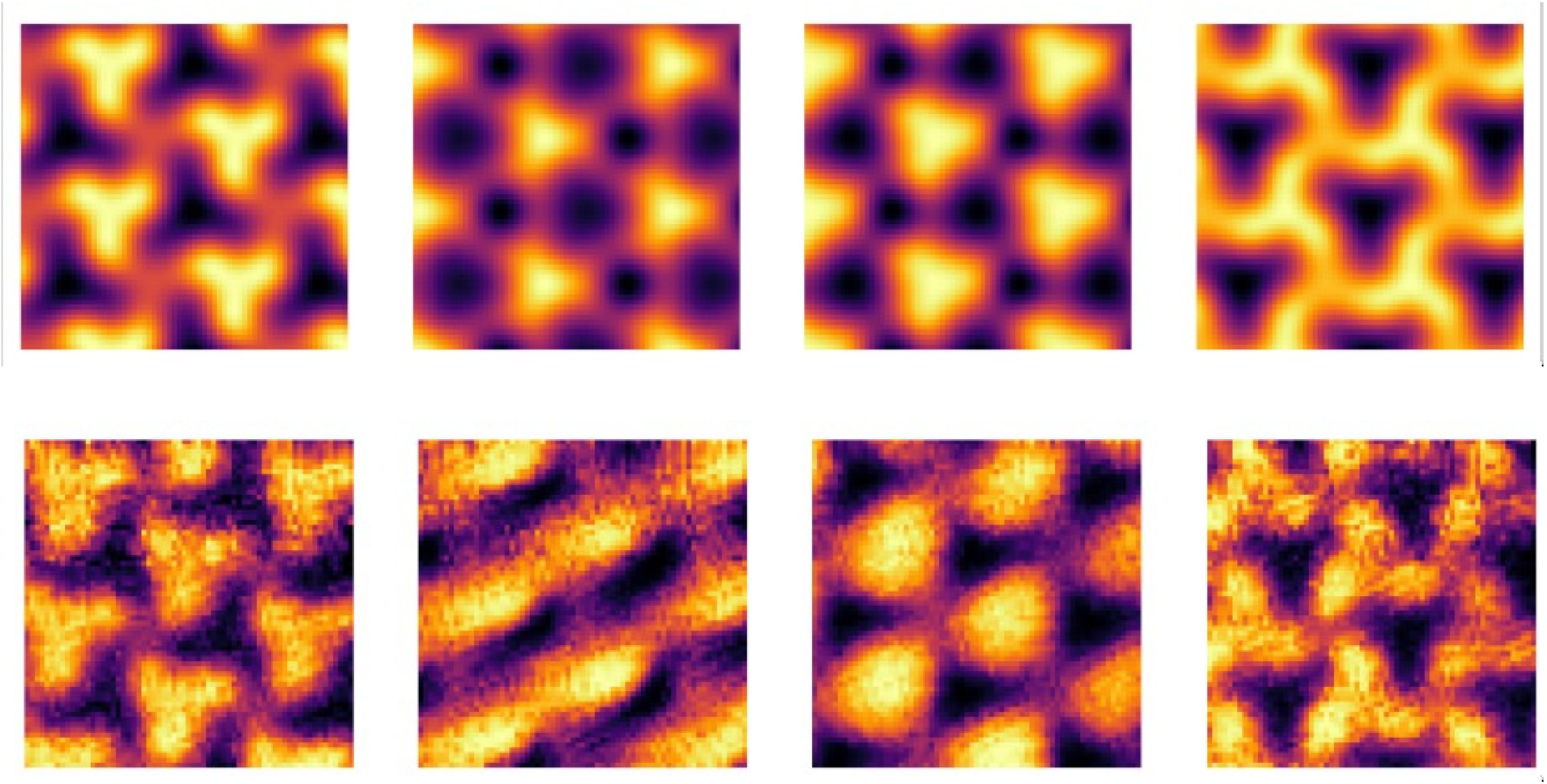

Preprocessing of the experimental data

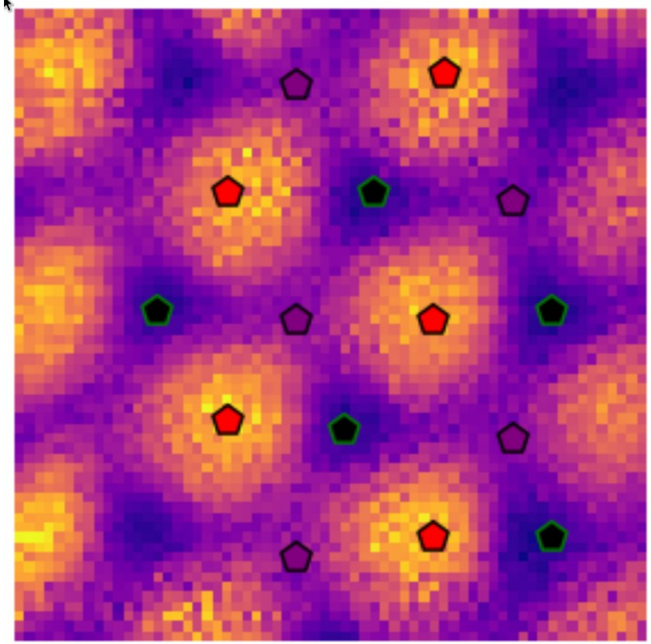

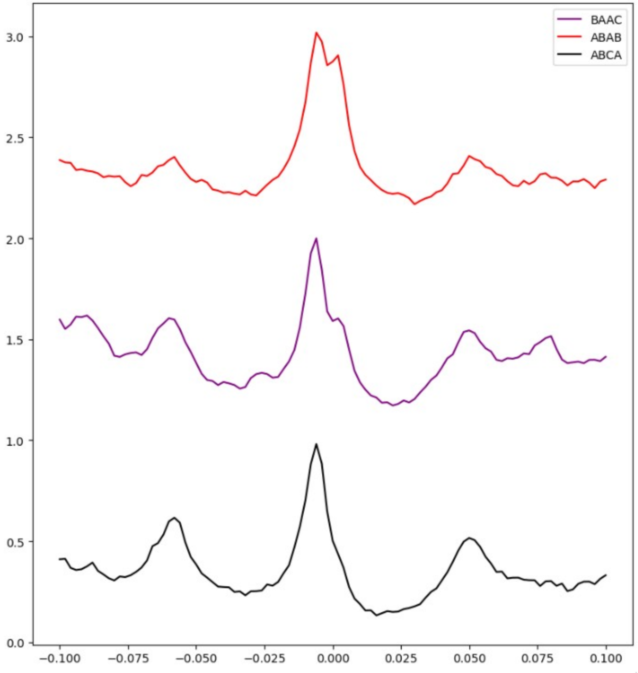

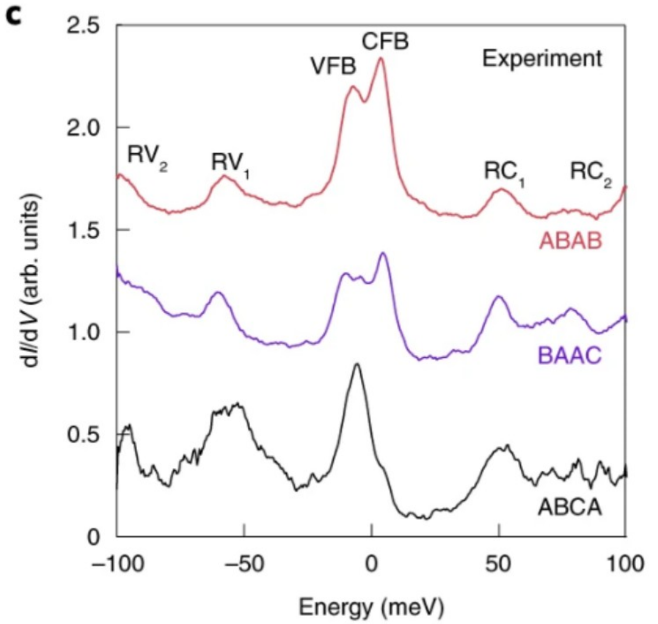

Preprocessing of the experimental data

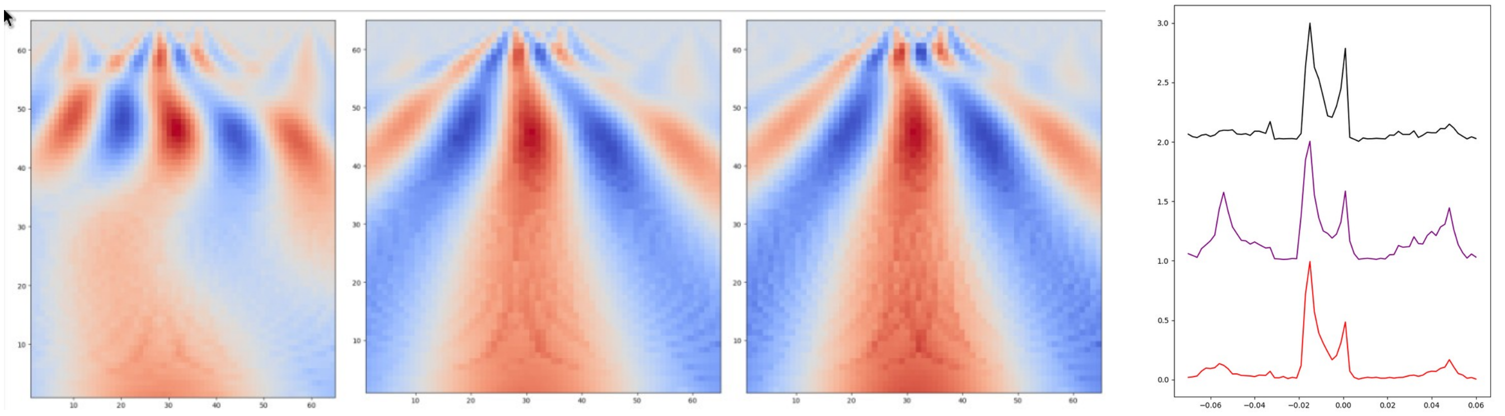

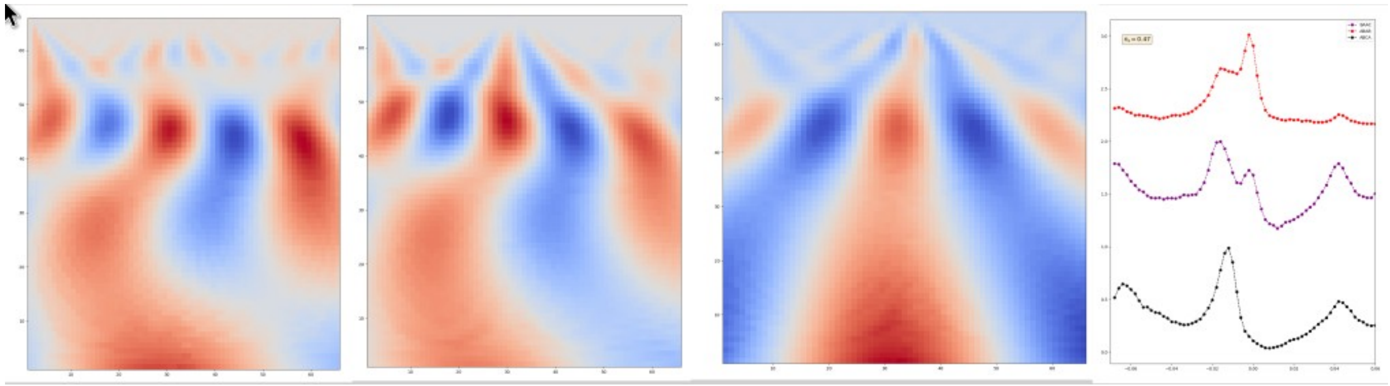

Predictions on D_{exp}

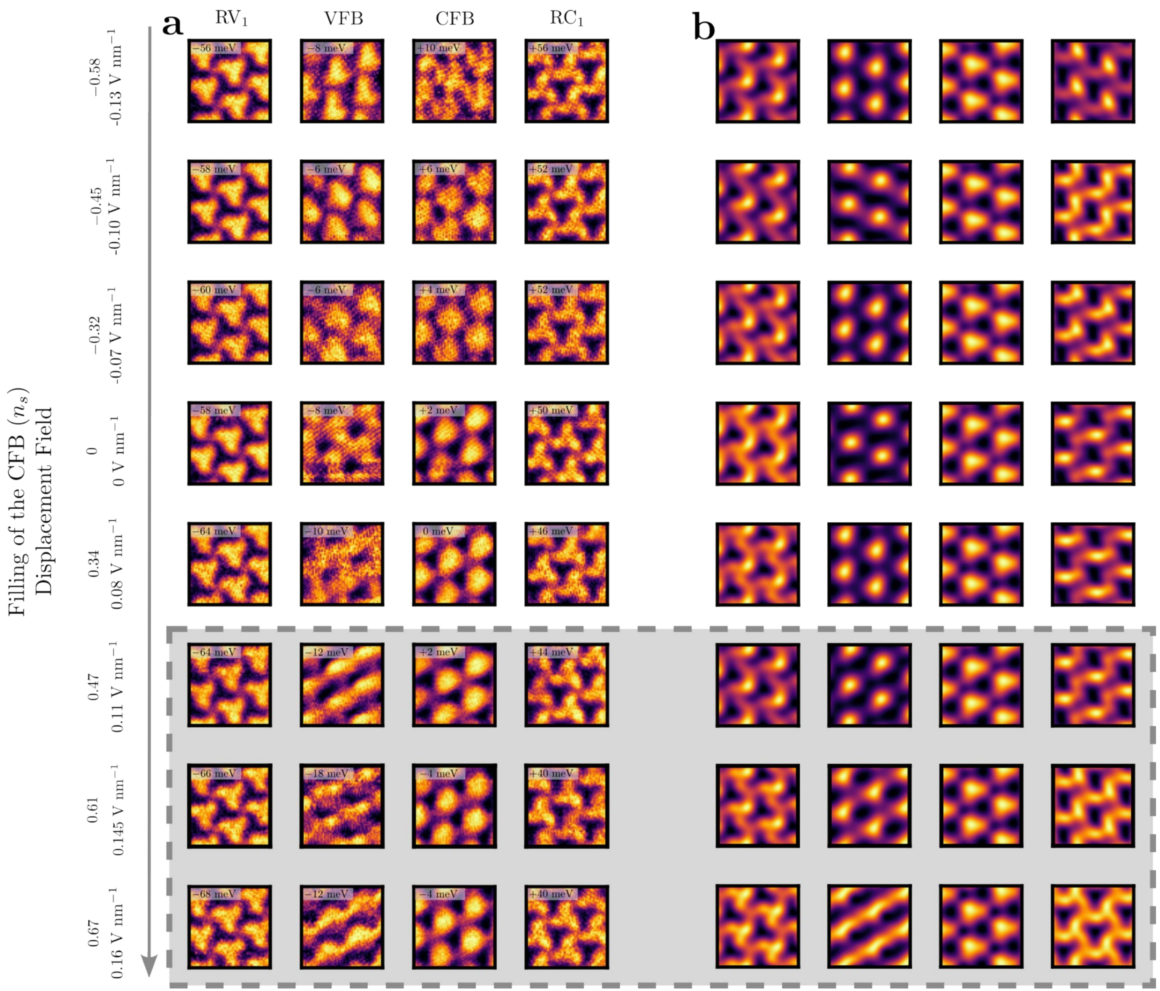

Preprocessing of the experimental data

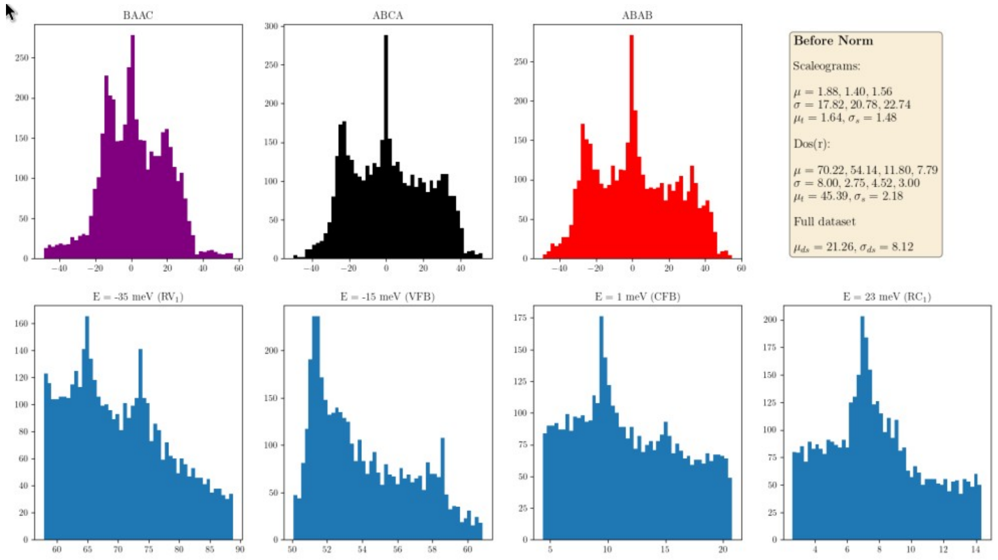

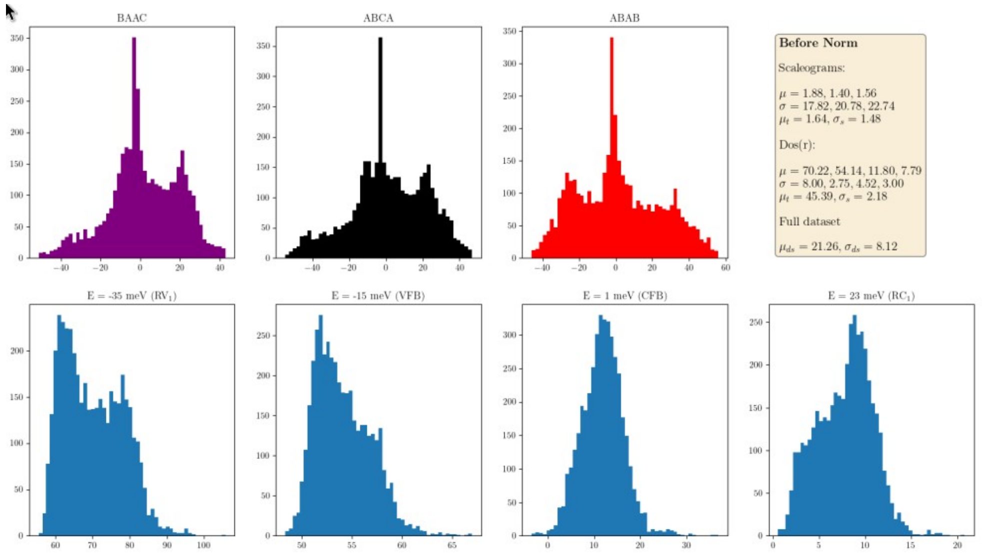

Limitations of theoretical model/data resolution

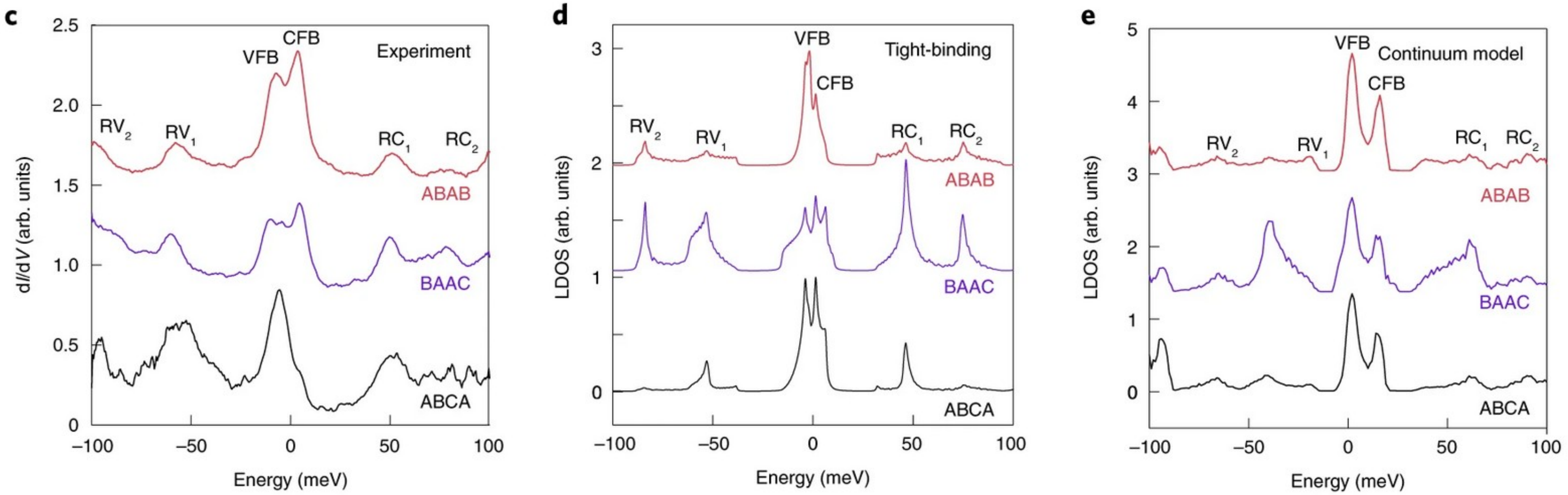

Interpretability? Correlations in AI nematic study

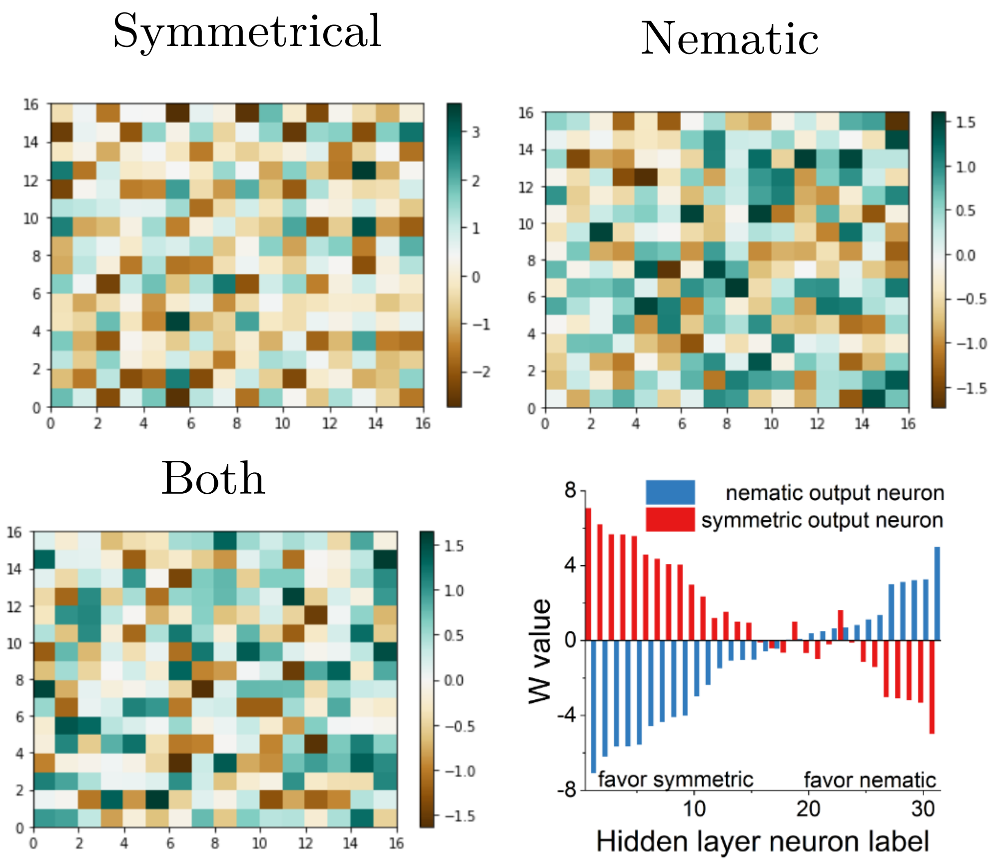

Goetz, J.B., et al **2020**. SciPost Physics, 8(6), p.087.

Tight Binding in TDBG

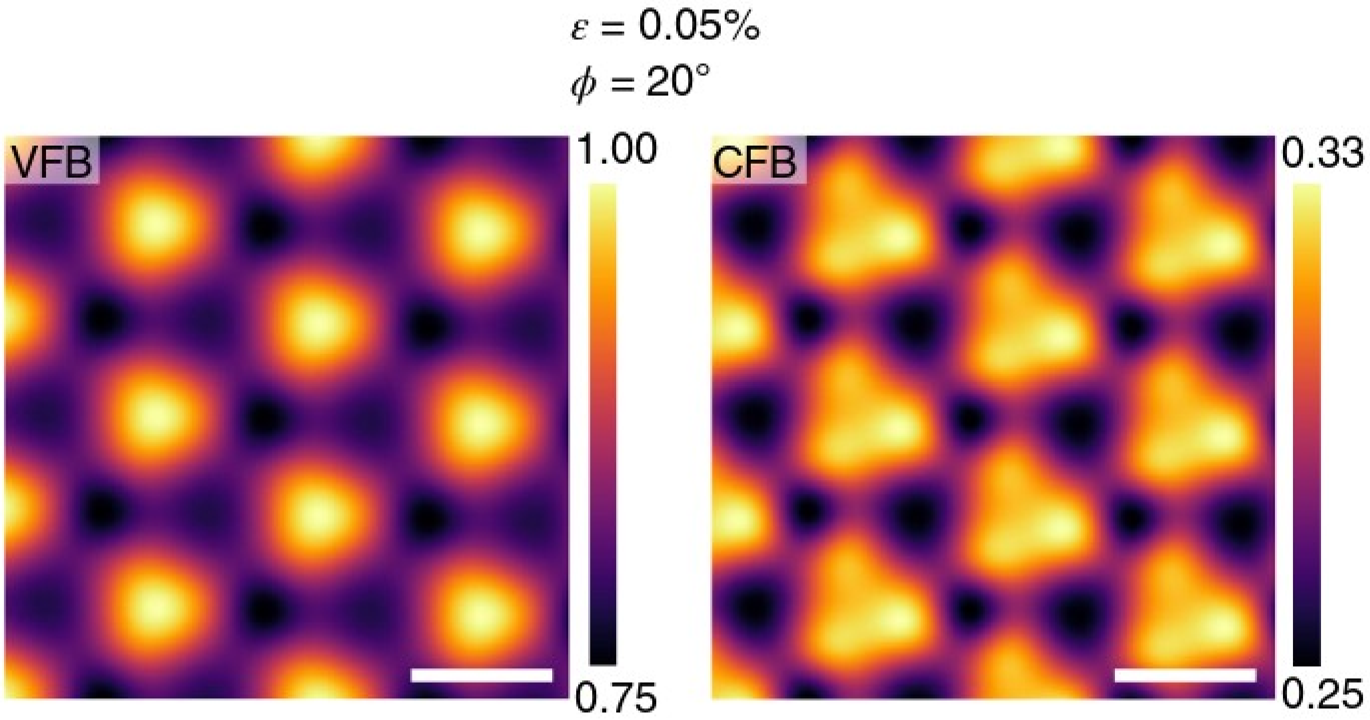

More nematic couplings: Intervalley GN

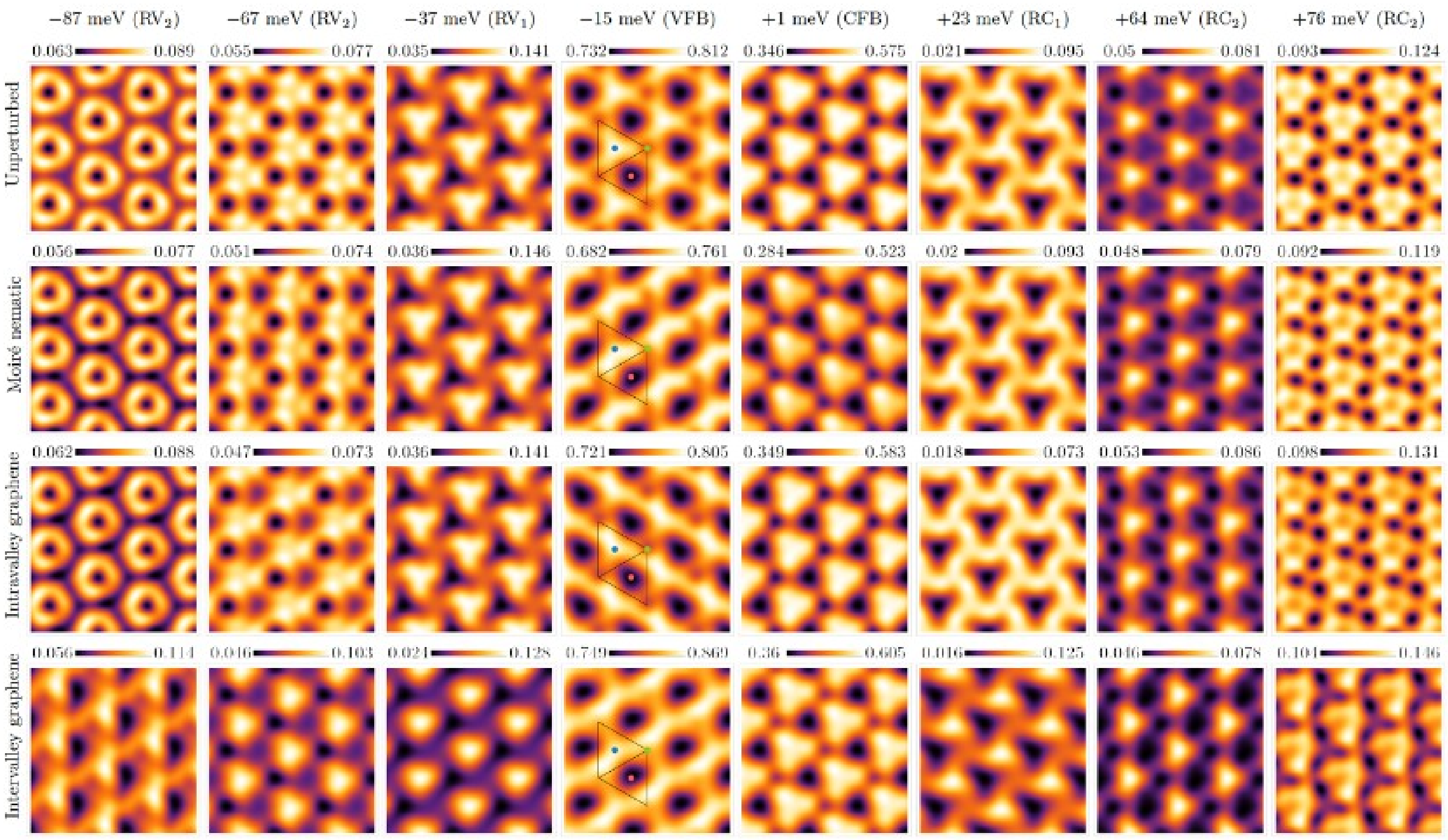

More nematic couplings: Intervalley GN

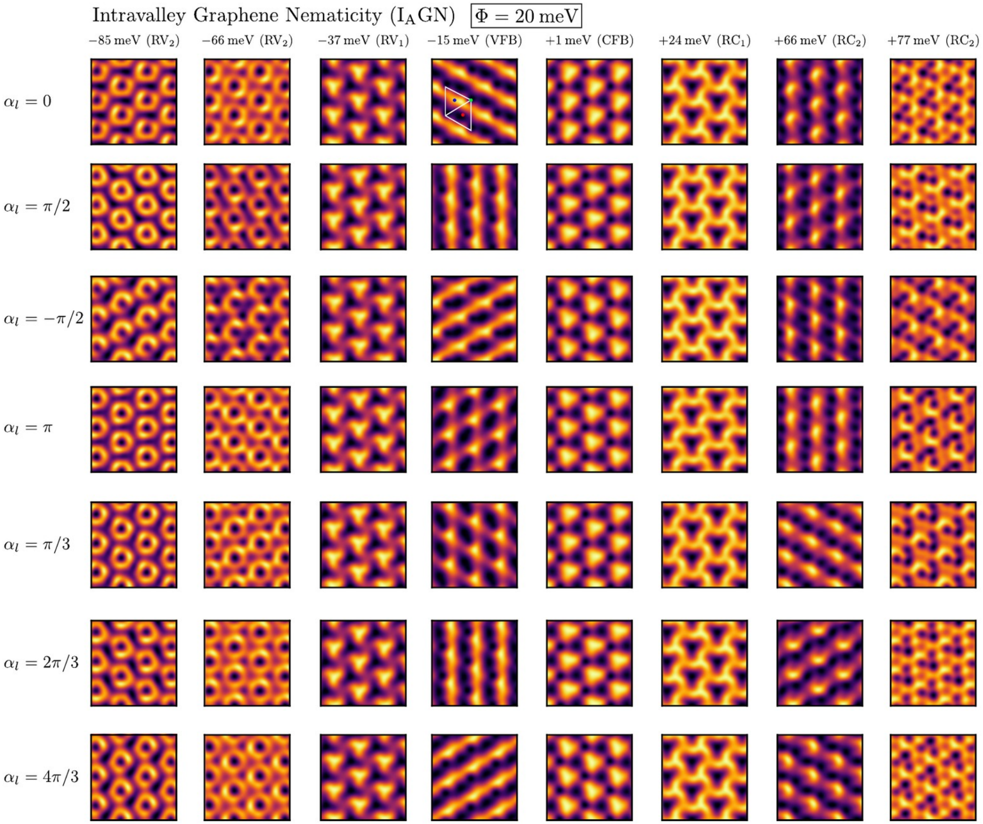

R. Samajdar, M. S. Scheurer, S. Turkel, et al. 2D Materials 8, 034005 (2021).